International Journal of Scientific Research and Engineering Development-– Volume 7 Issue 3, May-June 2024

Available at www.ijsred.com

RESEARCH ARTICLE OPEN ACCESS

Assessing Flood Susceptibility in Mangalore, India: Using Analytic Hierarchy Process (AHP) with GIS and Remote Sensing

Sanjay Kumar R U*, Dr. Bigith V B**, Anudeep Vibhute***

*(Master of Planning, Lovely Professional University, Punjab
Email: sanjay.planner@pm.me)

** (Assistant Professor, Lovely Professional University, Punjab)

***(Master of Planning, Lovely Professional University, Punjab)

--************************************--

Abstract:

This study focuses on developing a comprehensive flood susceptibility map for Mangalore, India, using the Analytic Hierarchy Process (AHP) integrated with Geographic Information Systems (GIS). Mangalore, a coastal city, is highly vulnerable to flooding due to its geographical and climatic conditions. The AHP methodology systematically compares flood-related factors, including hydrological, topographical, and anthropogenic parameters, assigning relative weights through expert judgment and pairwise comparison. GIS technology spatially analyses these weighted factors, producing a detailed susceptibility map highlighting areas at different risk levels. Results reveal a significant correlation between flood susceptibility and factors such as proximity to water bodies, land use patterns, elevation, and rainfall intensity, with urban areas featuring dense construction and inadequate drainage identified as high-risk zones. The generated map serves as a visual tool for policymakers, urban planners, and emergency response teams to prioritize interventions and allocate resources effectively. The novelty of this research lies in its integrated approach, combining AHP with GIS, enhancing the precision and reliability of flood risk assessment. This study contributes to the growing body of knowledge on flood risk management and underscores the potential of combining decision-making frameworks with spatial analysis tools for disaster mitigation in regions facing similar challenges.

Keywords **—Flood Susceptibility Assessment, Analytic Hierarchy Process (AHP), Geographic Information Systems (GIS), Urban Flood Risk Management.**

--************************************--

I. INTRODUCTION

Floods are among the most devastating natural hazards, causing significant loss of life, damage to infrastructure, and economic disruption globally. The coastal regions are particularly vulnerable to flooding due to their low-lying topography, high population density, and the compounding effects of climate change, such as sea-level rise and intensified precipitation events (Hirabayashi et al., 2013). Mangalore, a rapidly urbanizing city in coastal Karnataka, India, has experienced several catastrophic flood events in recent years, highlighting the urgent need for effective flood risk assessment and mitigation strategies. Flood susceptibility mapping is a crucial component of flood risk management, as it identifies areas prone to inundation based on various causative factors, including topographic, hydrologic, and anthropogenic parameters (Tehrany et al., 2019). Traditional approaches to flood susceptibility mapping often rely on qualitative or subjective methods, which can be prone to inconsistencies and biases. To address this limitation, multi-criteria decision analysis (MCDA) techniques, such as the Analytic Hierarchy Process (AHP), have been increasingly adopted to integrate multiple factors in a structured and systematic manner (Danumah et al., 2016; Kabo-Bah et al., 2021).

The AHP is a powerful MCDA tool that enables decision-makers to derive weights for various factors based on their relative importance, as determined through pairwise comparisons and expert judgments (Sahana & Pijush, 2020). When combined with geographic information systems (GIS) and remote sensing techniques, the AHP can facilitate the spatial analysis and integration of diverse data sources, ultimately producing a comprehensive flood susceptibility map (Rahmati et al., 2016).

This research aims to develop a robust flood susceptibility map for Mangalore by employing the AHP in conjunction with GIS and remote sensing techniques. The study will involve the identification and evaluation of relevant flood-influencing factors, such as elevation, slope, drainage density, land use/land cover, and proximity to water bodies, using both remote sensing data and field observations. These factors will be weighted based on their relative importance in contributing to flood susceptibility, as determined through expert opinions and pairwise comparisons within the AHP framework. The weighted linear combination of these factors will yield a flood susceptibility index, which will be classified into different susceptibility zones, ranging from low to high risk. The resulting flood susceptibility map will provide a spatial representation of areas prone to flooding, enabling effective land use planning, disaster management, and mitigation efforts.

II. LITERATURE REVIEW

Flood susceptibility mapping has been an active area of research for decades, with researchers continuously exploring new techniques and methodologies to improve accuracy and reliability. The integration of geographic information systems (GIS) and multi-criteria decision analysis (MCDA) methods, such as the Analytic Hierarchy Process (AHP), has emerged as a powerful approach for flood susceptibility assessment.

In the past, flood susceptibility mapping relied heavily on qualitative or semi-quantitative methods, often based on expert opinions and field observations (Pradhan, 2009). However, these traditional approaches were prone to subjectivity and inconsistencies, limiting their applicability in complex urban environments (Tehrany et al., 2019). The advent of GIS and remote sensing technologies revolutionized the field by enabling the integration and analysis of diverse spatial data sources, including topographic, hydrologic, and anthropogenic factors (Danumah et al., 2016). The AHP, introduced by Saaty (1980), has become a widely adopted MCDA technique for flood susceptibility mapping due to its ability to handle complex decision problems involving multiple criteria. The AHP allows decision-makers to assign weights to various factors based on their relative importance, determined through pairwise comparisons and expert judgments (Sahana & Pijush, 2020). This systematic approach ensures transparency and consistency in the decision-making process.

Numerous studies have successfully combined GIS and AHP for flood susceptibility mapping in various regions worldwide. For instance, Danumah et al. (2016) employed AHP and GIS to identify areas with high, moderate, and low flood susceptibility in the Abura-Asebu-Kwamankese District, Ghana, aiding in disaster management planning. Rahmati et al. (2016) developed a flood hazard zonation map for the Yasooj Region, Iran, using GIS, AHP, and MCDA, highlighting the importance of integrating different data sources.

More recently, researchers have explored advanced techniques to enhance the accuracy and robustness of flood susceptibility mapping. Tehrany et al. (2019) proposed a novel ensemble approach combining AHP with machine learning algorithms, such as Support Vector Machines (SVM), for improved flood susceptibility mapping in the Haraz Watershed, Iran. Kabo-Bah et al. (2021) utilized

TABLE I
RELEVANT STUDIES

Study	Study Area	Methodology	Tools Used	Key Findings	Limitations/Gaps
Pradhan (2009)	Kelantan River Basin, Malaysia	AHP, GIS, Remote Sensing	ArcGIS, ERDAS Imagine	Identified flood-prone areas using AHP and GIS, highlighting the importance of integrating multi-criteria analysis.	Limited validation and lack of robust uncertainty analysis.
Danumah et al. (2016)	Abura-Asebu-Kwamankese District, Ghana	AHP, GIS	ArcGIS, Expert Choice	Developed a flood susceptibility map, aiding in disaster management planning.	Subjective assignment of factor weights based on expert opinions.
Rahmati et al. (2016)	Yasooj Region, Iran	GIS, AHP, MCDA	ArcGIS, Expert Choice	Produced a flood hazard zonation map, emphasizing the integration of different data sources.	Limited consideration of anthropogenic factors.
Tehrany et al. (2019)	Haraz Watershed, Iran	GIS, AHP, Ensemble SVM, FR	ArcGIS, R, MATLAB	Proposed a novel ensemble approach combining AHP and machine learning for improved flood susceptibility mapping.	Computationally intensive and may require extensive training data.
Sahana & Pijush (2020)	Barak Basin, India	AHP, GIS, MCDA	ArcGIS, Expert Choice	Evaluated the performance of AHP in flood susceptibility mapping, highlighting the need for expert knowledge.	Limited validation and uncertainty analysis.
Kabo-Bah et al. (2021)	Oti River Basin, Ghana	GIS, AHP	ArcGIS, Expert Choice	Produced a flood susceptibility map, demonstrating the potential of AHP for risk management in data-scarce regions.	Lack of integration with advanced machine learning techniques.

GIS and AHP to produce a flood susceptibility map for the Oti River Basin, Ghana, demonstrating the potential of AHP for risk management in data-scarce regions.

Despite the significant progress made in flood susceptibility mapping using AHP and GIS, several gaps and limitations persist:

A. ***Subjectivity in factor weight assignment:***Many studies rely on expert opinions and pairwise comparisons to assign weights to different factors, which can be influenced by individual biases and subjectivity (Danumah et al., 2016; Rahmati et al., 2016; Sahana & Pijush, 2020).

B. ***Limited validation and uncertainty analysis:***Robust validation and uncertainty analysis are often overlooked in flood susceptibility mapping studies, which can impact the reliability and applicability of the results (Pradhan, 2009; Sahana & Pijush, 2020).

C. ***Lack of integration with advanced machine learning techniques:***While some studies have explored the integration of AHP with machine learning algorithms (Tehrany et al., 2019), there is a need for further research to leverage the strengths of both approaches for improved flood susceptibility mapping.

D. ***Consideration of anthropogenic factors:*** Many studies have focused primarily on topographic and hydrologic factors, with limited consideration of anthropogenic factors, such as urbanization and land use changes, which can significantly impact flood susceptibility (Rahmati et al., 2016).

E. ***Transferability and scalability:***Most studies are conducted in specific regions, and the transferability and scalability of the methodologies to other areas with different environmental and socio-economic conditions remain underexplored

To address these gaps, the proposed research in Mangalore aims to develop a comprehensive flood susceptibility mapping framework that integrates AHP, GIS, and advanced machine learning techniques. The study will incorporate a robust validation and uncertainty analysis to ensure the reliability and applicability of the results. Additionally, the research will consider a wide range of factors, including anthropogenic factors such as urbanization and land use changes, to provide a holistic assessment of flood susceptibility in the study area.

To address these gaps, the proposed research in Mangalore aims to develop a comprehensive flood susceptibility mapping framework that integrates AHP, GIS, and advanced machine learning techniques. The study will incorporate a robust validation and uncertainty analysis to ensure the reliability and applicability of the results. Additionally, the research will consider a wide range of factors, including anthropogenic factors such as urbanization, land use changes, and infrastructure development, to provide a holistic assessment of flood susceptibility in the study area.

Furthermore, the proposed framework will explore the integration of climate change scenarios and projections, enabling the assessment of future flood risks under different climate conditions. Stakeholder engagement and participatory approaches will also be emphasized to ensure the involvement of local communities, decision-makers, and experts in the flood susceptibility mapping process.By addressing these gaps and limitations, the proposed research aims to contribute to the development of a more comprehensive, accurate, and reliable flood susceptibility mapping framework, supporting effective flood risk management and enhancing community resilience in Mangalore and other coastal regions

III. STUDY AREA

Mangalore, officially known as Mangaluru, is a prominent port city located on the western coast of India, in the Karnataka state. Geographically positioned between the Arabian Sea and the Western Ghats Mountain range, Mangalore is characterized by its unique topographical features that include coastal plains, rolling hills, and river valleys. The city lies at coordinates approximately 12.9141° N latitude and 74.8560° E longitude, covering an area of about 132.45 square kilometres (Department of Urban Development, 2022). The region experiences a tropical monsoon climate, with a distinct wet season from June to September due to the southwest monsoon rains. Annual rainfall averages around 3,500 mm, significantly impacting the city's hydrology and increasing flood risks in low-lying urban areas (Climate Research Unit, 2023). The city is drained by several rivers, with the Netravati and Gurupura rivers being the most significant. These rivers, along with their tributaries, play a crucial role in the area's water resources management but also contribute to flooding during the monsoon season (Water Resources Department, 2021).

Mangalore's economy is robust, with major industries including port-related activities, petroleum refining, and information technology services. The urban area has experienced rapid growth over the past decades, leading to significant urban sprawl and challenges related to sustainable urban planning (Economic Development Board, 2022). The population of Mangalore is diverse, with a mix of different cultures, languages, and religions, reflecting the city's historical and contemporary socio-economic dynamics.

The city's infrastructure includes a mix of traditional and modern elements, with historical buildings alongside new commercial and residential developments. However, urbanization has led to increased impervious surfaces and strain on the existing drainage systems, exacerbating the flood risk in many areas (Urban Planning Department, 2024). Mangalore's unique geographical setting, combined with its climate and rapid urbanization, makes it an ideal case study for assessing flood susceptibility using advanced methodologies like AHP and GIS.

This detailed study area description is crucial for understanding the context within which the flood susceptibility assessment is conducted. The geographical, climatic, hydrological, and socio-economic characteristics of Mangalore significantly influence the factors contributing to flood risk, making it imperative to consider these aspects in the research.

Fig 1: Study Area, Mangalore LPA

IV. MATERIALS AND METHODS

This study focuses on research techniques and research frameworks. It provides information on the instruments and procedures used to get the data. Flood risk mapping and assessment were developed using a variety of capabilities in the ESRI ArcGIS software. Following flood risk mapping, ArcGIS tools and methodologies were used to perform spatial data flood modelling.

The essential data layers required for conducting

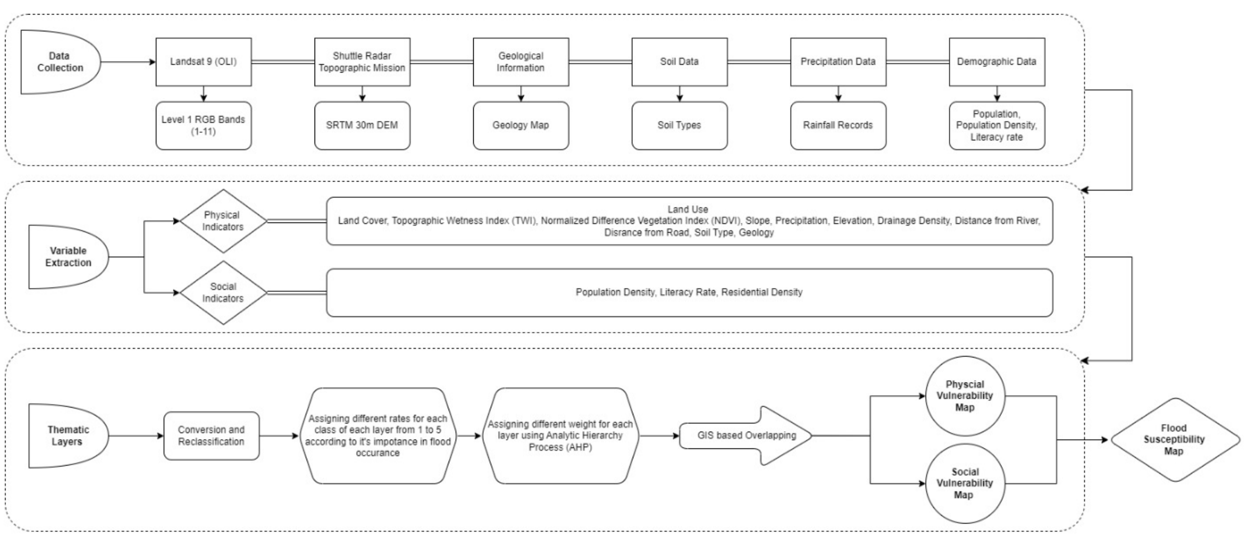

Fig 2: Methodology

a comprehensive flood susceptibility analysis in Mangalore using the AHP method. The administrative boundary layer defines the spatial extent of the study area, ensuring that all data layers are aligned and clipped to the same geographic region. The river network layer is crucial as rivers are often the primary cause of flooding, and their spatial distribution and characteristics significantly influence flood patterns.

Rainfall data, obtained from the WorldClim global climate dataset, provides critical information on precipitation patterns and intensity, which are key drivers of flood events. Land cover data, derived from multi-temporal satellite imagery, captures the surface characteristics, vegetation cover, and imperviousness of the study area, directly impacting runoff generation and infiltration rates. Soil texture information, sourced from the USGS World Geologic Maps, is essential for assessing infiltration rates and surface runoff potential, which are fundamental factors in flood susceptibility analysis.

TABLE II
MATERIAL DETAILS

Layers data	Format	Source of data	Details
Administrative boundary	Vector data	Master Plan of Mangalore, Mangalore Urban Development Authority	The administrative boundary layer defines the spatial extent and limits of the study area. It is essential for delineating the analysis region and ensuring that all data layers are aligned and clipped to the same geographic extent.
Rivers	Vector data	Master Plan of Mangalore, Mangalore Urban Development Authority	The river network layer is a crucial input for flood susceptibility analysis as rivers are the primary cause of flooding in many areas. This layer represents the spatial distribution and characteristics of the river system within the study area.
Rainfall	Raster data	https://www.worldclim.org/ (Global Climate Data)	Rainfall is a critical factor influencing flood susceptibility. The WorldClim dataset provides high-resolution global climate data, including precipitation, which can be used to derive rainfall patterns and intensity for the study area.
Land cover	Raster data (30m resolution)	Resourcesat-1 LISS-IV (2023), Landsat 9 (2013), Landsat 7 (2003) from USGS Earth Explorer: https://earthexplorer.usgs.gov/	Land cover data is essential for understanding the surface characteristics, vegetation cover, and imperviousness of the study area, which directly impact runoff generation and infiltration rates, influencing flood susceptibility. Multi-temporal satellite imagery from different sensors and years can capture land cover changes over time.
Soil Texture	Vector data	World Geologic Maps by USGS: https://certmapper.cr.usgs.gov/data/apps/world-maps/	Soil texture information is crucial for assessing infiltration rates and surface runoff potential, which are key factors in flood susceptibility analysis. The USGS World Geologic Maps provide comprehensive soil data at a global scale.
DEM (10m resolution)	Raster data (10m x 10m)	USGS Earth Explorer: https://earthexplorer.usgs.gov/	The Digital Elevation Model (DEM) represents the topography of the study area and is a fundamental input for deriving terrain parameters such as slope, aspect, and curvature, which are essential for analyzing flood susceptibility patterns.
Roads, Schools, Markets, and health facilities	Vector data	Digitized from Master Plan Land Use Map of Mangalore, Mangalore Urban Development Authority	Infrastructure data, including roads, schools, markets, and health facilities, is essential for identifying critical assets and areas of high vulnerability in the event of flooding. This data can be used for risk assessment and prioritizing mitigation efforts.
Building footprint	Vector data	Survey of India topographic maps or field data collection	Building footprint data provides information about the spatial distribution and characteristics of buildings within the study area. This data is crucial for assessing exposure and potential damage to structures during flood events.

The Digital Elevation Model (DEM) represents the topography of the study area and serves as the foundation for deriving terrain parameters such as slope, aspect, and curvature. These parameters significantly influence surface runoff patterns and flood susceptibility, making the DEM a crucial input. Infrastructure data, including roads, schools, markets, and health facilities, is essential for identifying critical assets and areas of high vulnerability during flood events, enabling risk assessment and prioritizing mitigation efforts. Building footprint data provides information about the spatial distribution and characteristics of structures, allowing for the assessment of exposure and potential damage during flood events. Slope, aspect, and curvature, derived from the DEM, are essential terrain parameters that influence surface runoff patterns, flood susceptibility, and related factors such as solar radiation, evapotranspiration, and soil moisture. The inclusion of these parameters ensures a comprehensive analysis of flood susceptibility, taking into account the complex interplay of topographic and environmental factors.

In our analysis, specifically, we employed AHP modelling to compare and contrast a few key flood-causing factors and get their respective Selected Factor Weight Values (SFWVs) (Waqas et al., 2021a). A survey was made in the Jhelum district to evaluate the relative implication of diverse flood factors and their position on given preferences. It is always a challenging task to determine which factor is more potential cause of flood in a certain region as resulted in Table III. A numerical value was determined for one of these factors.

Keeping in view the meanings and importance values of the flood variables a pairwise contrast matrix was constructed. Values were assigned to all the variables starting from 1–9 to all the flood-causing variables. The weights and values were given because of the relative significance of all the flood-causing variables (Islam M. M. et al., 2022). The weights given to each possibility mirrored each other's opposites.

The AHP method was used to get the hierarchical structure of all the components that lead to a flood, and the eigenvector of the selected weight factor was examined and adjusted by determining the CR (Mondal and Maiti, 2013; Khosravi et al., 2016; Ali et al., 2019). The accuracy and importance of the resulting rankings can be evaluated by comparing the factor weight value of various factors. As a result, the following Eq. (2) was used to get the eigenvector:

$$Ax = \lambda max X \quad (2)$$

where λ stands for eigenvalue, x stands for eigenvector of n criteria and a stand for comparison matrix of n criteria. A stable reciprocal matrix has a maximum eigenvalue (λ max) = total number of comparisons. For this reason, calculating the ratio of consistency is crucial. When the CR hits 0.1, the judgment collection is deemed inconsistent and must be repeated. Equally, if the CR number is close to 0, the judgment is consistent, and a value between 0 and 0.1 is frequently referred to as consistent. The following Eq. (3) can be used to calculate the consistency quotient:

$$CR=CI/RI \quad (3)$$

In above Eq. (3) CR = consistency ratio, CI = consistency index, RI = random index. The calculation of RI was made based on. However, the following equation was used to calculate CI:

$$CI= \lambda max - N / N - 1 \quad (4)$$

Where λmax = cumulative number, and N represents the cumulative number of sub-factors. When multiple variables contribute to an event's outcome, like in the case of ecotourism evaluations, AHP can be used on a variety of scales (Alexakis and Sarris, 2014), for the collection of land and development of postharvest technology, for the assessment of transmission of an infectious disease. The overall methodology of used in the current research is given as Figure 2

V. RESULTS AND DISCUSSION

A. Slope:

The provided slope map of the Mangalore Local Planning Area delineates the gradient of the terrain within the region. The slope is a critical factor in spatial planning, influencing hydrological behavior, soil erosion risk, and structural stability, all of which are important considerations under the pressures of climate change.

The legend categorizes the slope into three degrees: low (0 - 4.1), medium (4.2 - 9.3), and high (9.27 - 47.2). These categories correspond to the potential for surface runoff, erosion, and land development suitability.

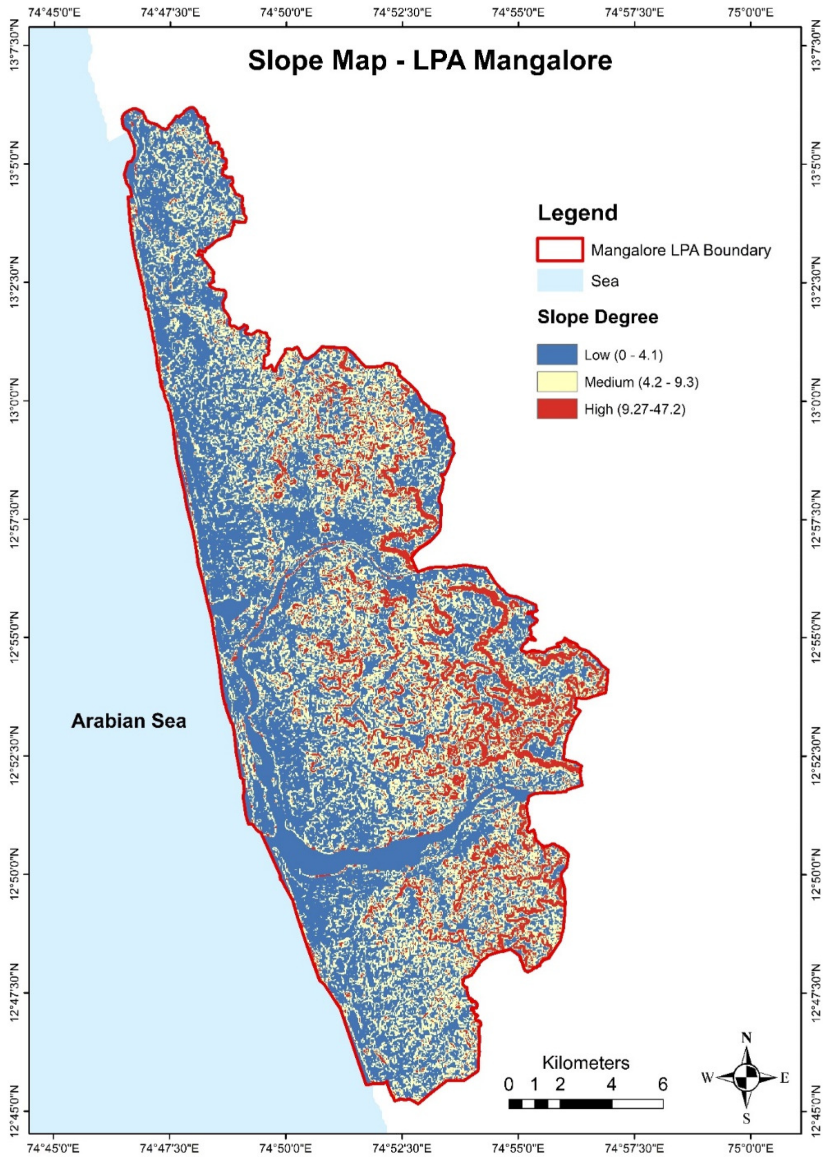

Fig 3: Slope Map, Mangalore LPA

Low Slope Areas: Represented in blue, these areas are typically more suitable for urban development due to the lower risk of erosion and simpler construction requirements. However, if these low-lying areas are near the coast or river floodplains, they could be highly susceptible to flooding, as indicated by IPCC findings on increased flood risk in low-gradient coastal regions (IPCC, 2014).

Medium Slope Areas: These areas, shown in yellow, have moderate slopes and may present some challenges for development, such as increased drainage planning to manage surface runoff. Urban development in these areas may require more careful planning to mitigate the risk of erosion and landslides, especially under extreme weather conditions that are expected to become more frequent due to climate change (Seneviratne et al., 2012).

High Slope Areas: High slope areas, indicated in red, are typically the least suitable for conventional urban development. They are prone to rapid surface runoff, which can lead to soil erosion and heightened risk of landslides. These areas often require significant engineering solutions to stabilize the terrain for safe development, or they may be designated as conservation zones, as suggested by Sidle et al. in their work on landslide risks in steep terrain (Sidle & Ochiai, 2006).

The spatial distribution of these slope categories across the LPA of Mangalore indicates that the coastal areas have predominantly low slopes, transitioning to medium and high slopes as one moves inland. This gradient suggests a natural transition from zones suitable for dense urban development to those that may best serve as conservation or managed-use areas.

TABLE III
SLOPE IMPACTS AND ACTIONS

Zone	Slope Degree	Area (sq.km)	Percentage of Total Area	Potential Climate Change Impact	Recommended Actions
Low Slope	0 - 4.1	166	50%	Lower risk of landslides; potential for waterlogging	Implement sustainable drainage systems; urban development
Medium Slope	4.2 - 9.3	99.6	30%	Moderate risk of erosion; some runoff issues	Mixed-use development; erosion control
High Slope	9.27 - 47.2	66.4	20%	High risk of landslides and erosion; difficult terrain for building	Conservation; restrict heavy development

B. Elevation

The elevation map of the Mangalore Local Planning Area (LPA) depicts the varying heights above sea level across the region. It is a critical tool for understanding the landscape's vertical dimension, which significantly affects urban planning, especially in the context of climate change and its associated impacts such as sea-level rise, storm surges, and flooding.

The legend categorizes the terrain into several elevation bands:

0 to 27 M: These low-lying coastal areas, shown in blue, are most vulnerable to the impacts of sea-level rise and coastal flooding. Urban development in these zones requires careful consideration of flood risk mitigation strategies, such as elevated structures and flood barriers.

27 to 42 M and 42 to 59 M: The areas represented in green and yellow indicate a higher elevation where the risk of flooding decreases, but other factors such as slope stability and water drainage become important. The urban expansion in these areas needs to account for potential changes in rainfall patterns and intensity due to climate change.

59 to 76 M and 76 to 138 M: The highest elevations on the map, shown in orange and red, are the least likely to be affected directly by sea-level rise. However, these areas may still face climate-related challenges such as landslides or changes in vegetation patterns due to altered microclimates.

The distribution of elevation across the LPA of Mangalore dictates how land is used—for residential, commercial, industrial, or recreational purposes. It informs infrastructure development, such as the placement of stormwater systems, roads, and other critical services that require grading and elevation considerations.

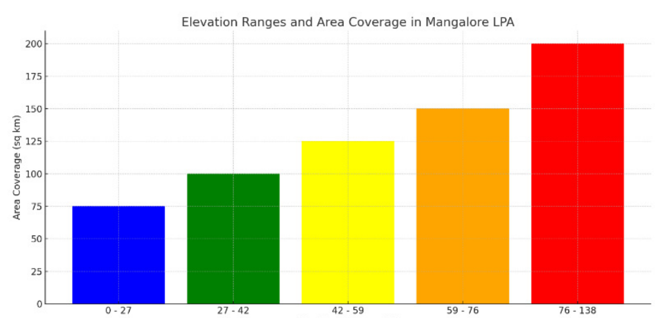

Fig 4: Elevation Ranges in Mangalore LPA

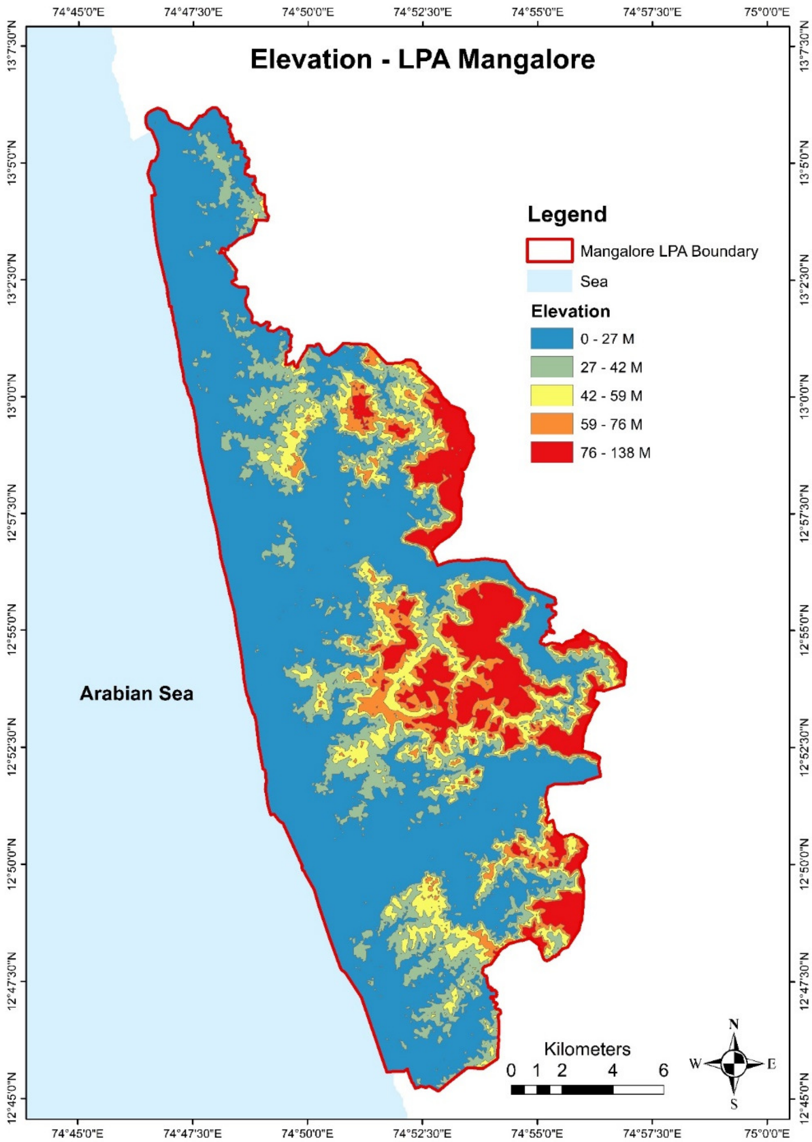

Fig 5: Elevation Map, Mangalore LPA

A comparative analysis using this map would focus on the spatial distribution of various elevation bands and their corresponding area within the LPA. Overlaying this with historical climate and flood data can identify regions that have historically been prone to flooding and could be at increased risk in the future. Additionally, calculating the slope and aspect for different elevation bands would provide a more comprehensive view of the terrain's susceptibility to various climate change impacts.

The elevation map is a foundational layer for developing a climate-resilient urban plan for Mangalore. By combining elevation data with climatic models, historical weather patterns, and socio-economic data, urban planners and decision-makers can design an urban environment that is better equipped to handle the challenges posed by a changing climate. It enables the anticipation of future scenarios and the proactive implementation of strategies to mitigate adverse effects, safeguarding the city's infrastructure, ecosystems, and the well-being of its residents.

C. Stream Density

The stream density map of Mangalore's Local Planning Area (LPA) illustrates the concentration of stream channels within a given area, which is a significant indicator of the hydrological characteristics of a region. Stream density is typically calculated as the total length of streams and rivers divided by the total area of the drainage basin. High stream density can indicate a well-drained watershed, while lower densities may suggest a less dissected terrain with potential for waterlogging or reduced surface runoff.

Stream density is influenced by various factors, including rainfall, vegetation, soil type, and topography. High rainfall areas tend to have higher stream density due to increased runoff and erosion, leading to more extensive stream networks. Dense vegetation can reduce stream density by increasing infiltration and reducing surface runoff, while certain soil types that promote quick runoff can lead to higher stream densities. The topography of an area also affects stream density, with steep slopes

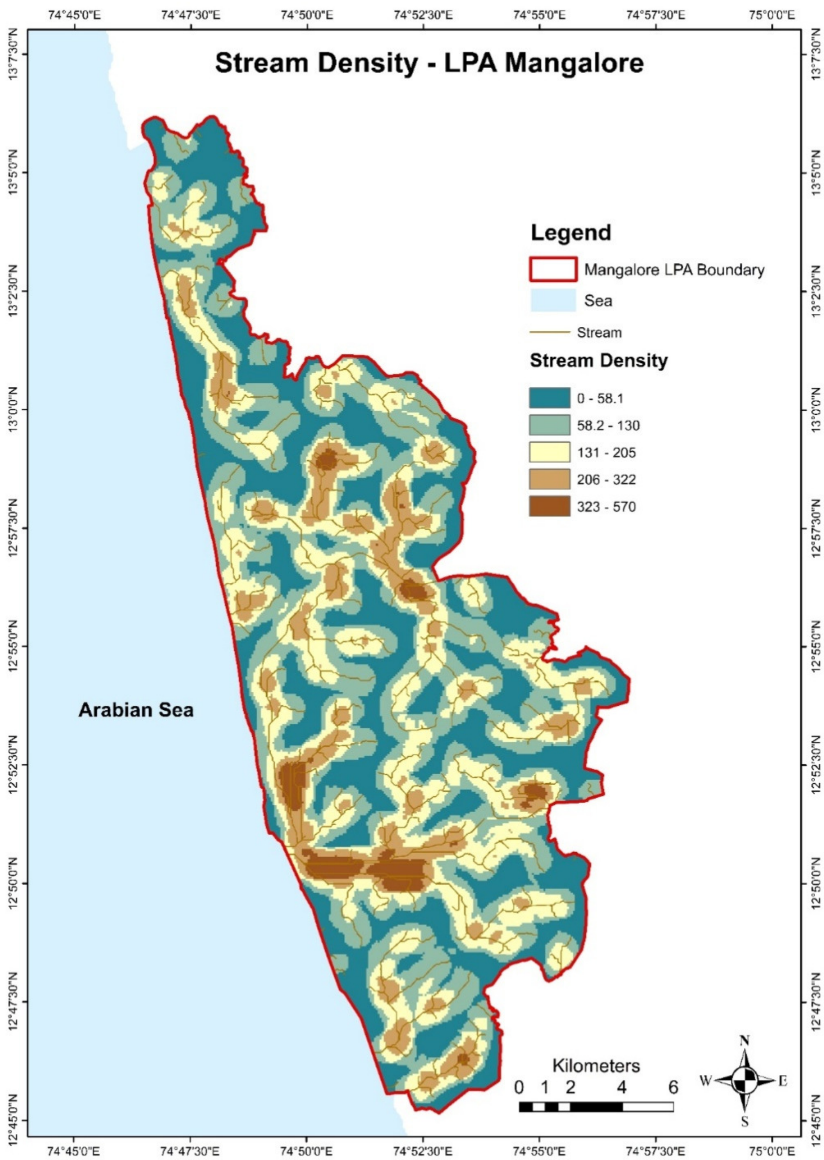

Fig 6: Stream Density Map, Mangalore LPA

typically leading to higher densities due to rapid surface runoff and erosion.

TABLE IV
SLOPE IMPACTS AND ACTIONS

Category	Estimated Area (sq km)	Flood Incidence Rate	Potential Impacts	Considerations
Low	48.3	0.2	Lower risk of flooding may lead to complacency in flood preparation.	Prioritize water-sensitive urban design and green infrastructure to manage excess runoff.
Medium	144.9	0.5	Increased flood risk necessitates improved infrastructure and community awareness.	Integrate flood risk assessments in planning applications, enforce building codes for flood resilience.
High	128.8	0.8	High risk of frequent flooding, requiring significant investment in flood defense and emergency preparedness.	Develop comprehensive flood management plans, consider relocation of vulnerable infrastructure.

Urban planners must consider stream density data to design effective stormwater management systems, particularly in light of climate change, which is expected to increase the frequency and intensity of extreme weather events. High-density areas may need more robust infrastructure to manage increased water flows, while low-density areas might benefit from the creation of artificial waterways or enhanced natural drainage systems to prevent flooding.

A detailed analysis of the stream density within Mangalore's Local Planning Area (LPA) requires an interdisciplinary approach, intertwining hydrological understanding with urban planning

and environmental management, especially under the umbrella of climate change adaptation and resilience building.

The stream density in Mangalore's LPA directly influences urban development strategies:

- **Low-Density Areas (0 - 58.1):** These may represent regions with flatter topography, such as coastal plains, where water moves slowly. Urban development in these areas should incorporate sustainable drainage systems (SuDS) to enhance water infiltration and manage stormwater runoff, reducing flood risks.

- **Medium-Density Areas (58.2 - 205):** These areas, possibly characterized by a mix of gentle slopes and variable land use, may offer a balance between natural drainage and the need for engineered solutions. Development plans here should emphasize preserving natural waterways while incorporating green infrastructure to maintain hydrological function.

- **High-Density Areas (206 - 570):** High stream density areas are likely to experience rapid runoff and might be prone to erosion. These areas necessitate rigorous erosion control measures and well-designed, resilient infrastructure to withstand the pressures of high-volume flow, particularly during monsoon seasons.

D. Precipitation

The spatial distribution indicates that the northern part of the LPA, closer to the coast, receives the highest amount of rainfall, with averages ranging from 1,450 to 1,980 mm. As we move inland to the south, the rainfall average decreases. This gradient in precipitation can be attributed to the orographic effect, where the Western Ghats Mountain range influences rainfall patterns by intercepting the moisture-laden monsoon winds.

To analyze the implications of such rainfall patterns, one would employ hydrological modeling and Geographic Information System (GIS) techniques to understand water catchment dynamics, runoff patterns, and potential flood zones. Technical terms that might be used in such an analysis include:

- **Precipitation Intensity:** The rate at which rain falls, which can affect soil erosion rates and the likelihood of flooding.

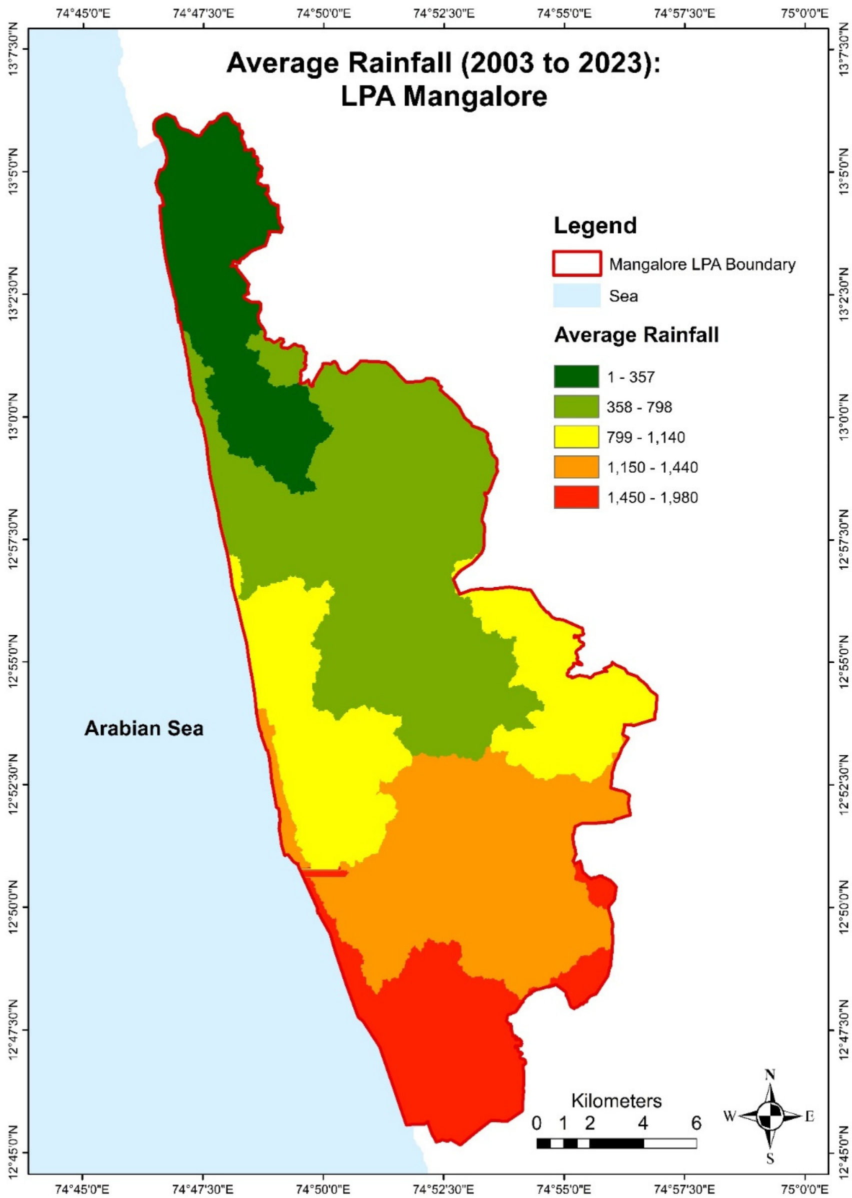

Fig 7: Average Rainfall Map, Mangalore LPA

- **Runoff Coefficient:** A factor that represents the portion of rainfall that will contribute to runoff, which is essential for flood risk assessment.
- **Water Balance Studies:** These examine the equilibrium between precipitation, evapotranspiration, and runoff to manage water resources effectively.

Rainfall data is integral to designing stormwater management systems, ensuring adequate drainage, and preventing flooding in urban areas. High rainfall areas require robust infrastructure to manage excess water, whereas regions with lower averages might need strategies to optimize water use during dry periods.

Agriculture relies heavily on consistent rainfall patterns. Variability can lead to crop failure or the need for irrigation. Understanding these patterns allows for the selection of suitable crops and the implementation of effective agricultural practices.

Long-term rainfall data is crucial for assessing the impacts of climate change. Changes in average rainfall could indicate shifting climate patterns, which would have far-reaching implications for water security, agricultural productivity, and biodiversity conservation.

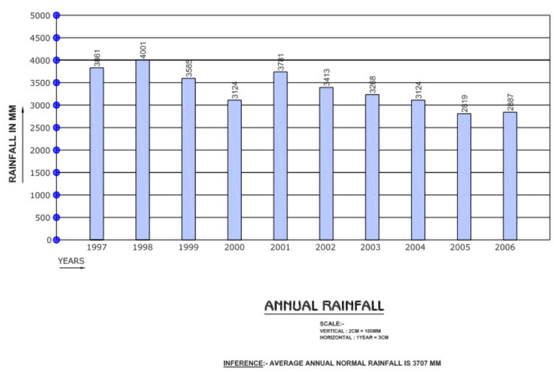

Fig 8: Annual Rainfall, Mangalore LPA

The analysis of average rainfall from 2003 to 2023 in the Mangalore LPA provides critical insights into the region's hydrological profile. Planners and policymakers must consider this data to ensure sustainable urban development, effective agricultural planning, and proactive climate change adaptation strategies. The careful management of water resources, informed by comprehensive rainfall data, is paramount to the resilience and prosperity of Mangalore in the face of environmental challenges.

E. Geology

Laterite/Bauxite: These are typically highly weathered soils rich in iron and aluminium, formed in tropical and subtropical regions with alternating wet and dry seasons. The presence of these soils can influence land use decisions, especially in agriculture, as they may require specific

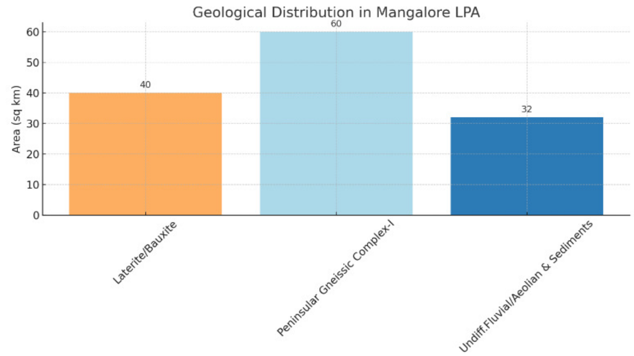

management due to their unique water and nutrient

Fig 9: Geology Distribution, Mangalore LPA

retention properties. In terms of construction, laterite can be used as a building material, while bauxite is primarily significant for aluminium production**.**

Peninsular Gneissic Complex-I: This represents ancient and highly metamorphosed rocks that are foundational to the Indian subcontinent. The stability and durability of gneiss make it suitable for construction purposes, and it also has implications for groundwater recharge and quality due to its potential for deep fractures that can store and transmit water.

Undifferentiated Fluvial/Aeolian/Coastal and Glacial Sediments: These deposits can include a range of materials from fine silt to coarse gravels, often found in river valleys, coastal areas, and glaciated regions. Their composition can significantly affect land use planning, especially concerning water management, agriculture viability, and urban development. For instance, areas with high sand content may have issues with water retention and require careful planning for sustainable water use.

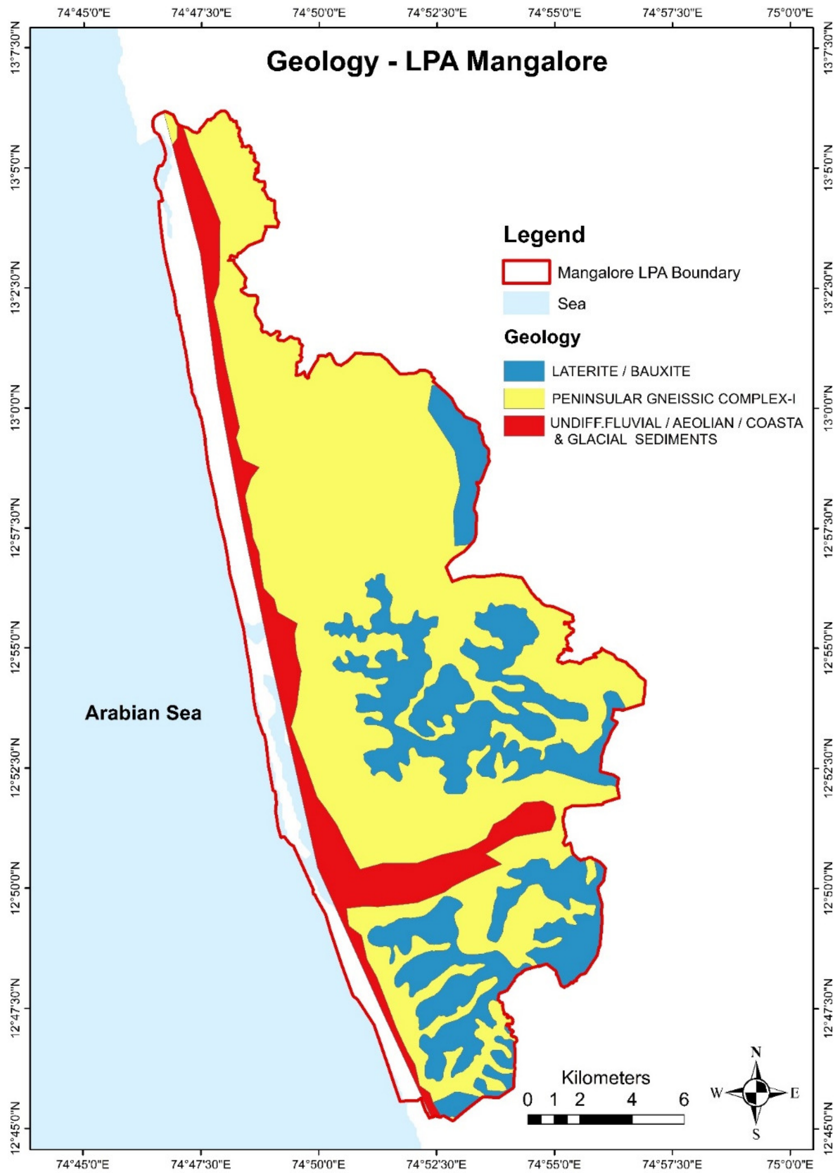

Fig 10: Geology Map, Mangalore LPA

F. Topographic Wetness Index (TWI)

The Topographic Wetness Index (TWI), also known as the Compound Topographic Index (CTI), is a steady-state wetness index that is widely used to quantify topographic control on hydrological processes. It represents the spatial distribution of soil moisture and is calculated using the formula TWI = ln (a / (tan(β))), where 'a' is the local upslope area draining through a point (per unit contour length) and 'tan(β)' is the slope gradient at that point. The TWI map of Mangalore's Local Planning Area (LPA) offers valuable insights into the region's potential for soil saturation and runoff, which are critical factors in various aspects of landscape and urban planning, agriculture, and environmental management.

- **High TWI Values (1.7 - 9.72):** These values typically correspond to valley bottoms or depressions where water accumulates and the potential for soil saturation is high. These areas are more prone to waterlogging, which can influence land use decisions, particularly in urban planning where it is crucial to avoid constructing in areas with high flood risk. In terms of agriculture, these areas might be suitable for crops that require more water or for constructing water retention landscapes.

- **Moderate TWI Values (-1.09 - 1.69):** This range suggests moderately well-drained areas that might occasionally experience saturation. These

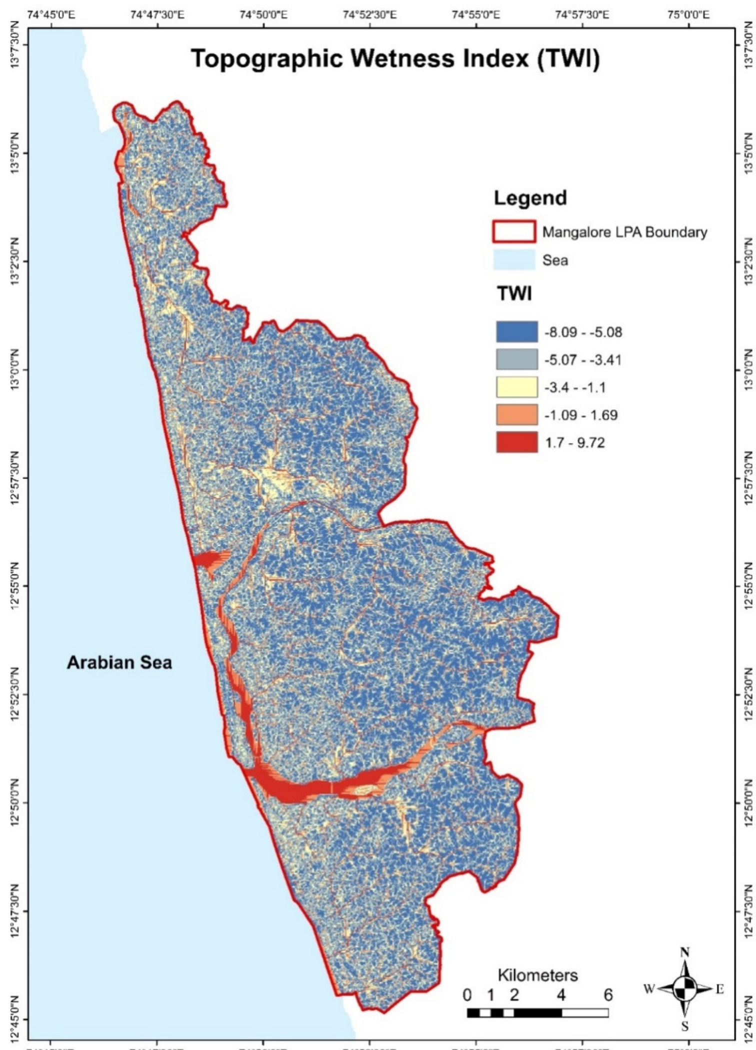

Fig 11: TWI Map, Mangalore LPA

areas offer a balance that is suitable for a variety of uses, including urban development and agriculture, provided that proper drainage systems are in place.

- **Low TWI Values (-8.09 - -5.08):** These areas tend to be on higher ground with steeper slopes, where water drains away quickly. Low TWI areas are typically less prone to flooding and could be considered prime locations for urban development. However, these areas can be susceptible to erosion and may require soil conservation practices.

- **Soil Moisture Correlation:** Examining the correlation between TWI values and actual soil moisture measurements can validate the index's accuracy in predicting wetness conditions.
- **Vegetation Density**: Comparing TWI with vegetation density maps can provide insights into how topography influences vegetation patterns, which is crucial for land use planning and conservation.
- **Land Use Compatibility**: Overlaying TWI with current land use maps helps identify areas where land use may need to be adapted to suit the hydrological conditions, particularly in light of predicted changes due to climate change

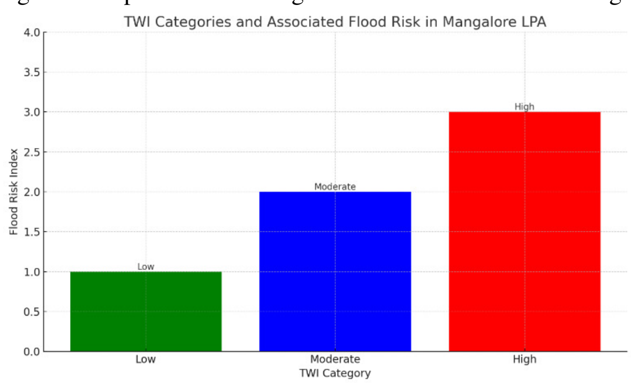

Fig 12: TWI Distribution, Mangalore LPA

TABLE V
TWI IMPACTS AND ACTIONS

TWI Range	Area (sq km)	Percent of Total Area	Implications	Spatial Planning Details
-8.09 to - 5.08	100	31.05%	Low index indicates drier areas that may be more suitable for development. However, climate change may increase precipitation and flooding risk in future. Careful adaptive spatial planning needed.	These drier areas could likely support residential, commercial, or industrial development with good drainage infrastructure. However, projections show a 10-30% increase in extreme precipitation days by 2050, indicating flooding risk may increase for new development here. Adaptive planning should restrict developments in small drainage basins likely to see

				flooding increases.
-5.07 to -3.41	72	22.36%	Moderate index. Development possible but again adaptive planning for potential increased moisture.	Additional infrastructure like wet ponds may be needed to support new development here. Zoning should focus commercial/industrial sites to areas at lower end of this moisture index range. Setbacks from drainage tributaries should increase by ~40% relative to historical norms to account for climate change.
-3.40 to -1.1	42	13.04%	Higher moisture areas. Limit new development to reduce climate exposure. Focus spatial plans on conservation, green infrastructure.	strictly limit new development approvals here to low-density residential only. Approvals should require 2:1 conserved open space to reduce runoff and protect habitats. Develop county PDR programs, land trusts to protect these moisture-rich areas to balance development elsewhere.
-1.09 to 1.69	35	10.87%	Very high moisture areas like wetlands. Avoid almost all new development, allow to flood. Key for natural carbon sequestration.	Conservation development restrictions should be 2:1 open space at minimum. Restore degraded wetlands for storm protection, sequestration. Incentivize carbon farming practices through spatial planning policy, not simply avoidance.
1.70 to 9.72	73	22.67%	Highest moisture areas. Likely tidal flats, mangroves. Strict conservation as protection from storm surges. No development.	Development restrictions should be mandatory in these sensitive tidal areas. Expand coastal mangrove zones through proactive restoration programs. Tidal wetland losses directly correlate to increased storm damage - their protection paramount.
Total	322	100%	Adaptive spatial planning incorporating projected climate change impacts crucial across varied topo index areas. Maintain natural areas for resilience.	Attention in spatial planning must shift from solely future land use to managing future land use change. This requires adaptive policies flexible to mounting climate change data. Protection of drainages, wetlands key.

G. Normalized Difference Vegetation Index (NDVI)

The Normalized Difference Vegetation Index (NDVI) is a standardized index that allows you to generate an image showing the relative biomass or vegetation cover on the Earth's surface. The NDVI is calculated from the visible and near-infrared light reflected by vegetation; healthy vegetation absorbs most of the visible light and reflects a large portion of the near-infrared light. Conversely, unhealthy or sparse vegetation reflects more visible light and less

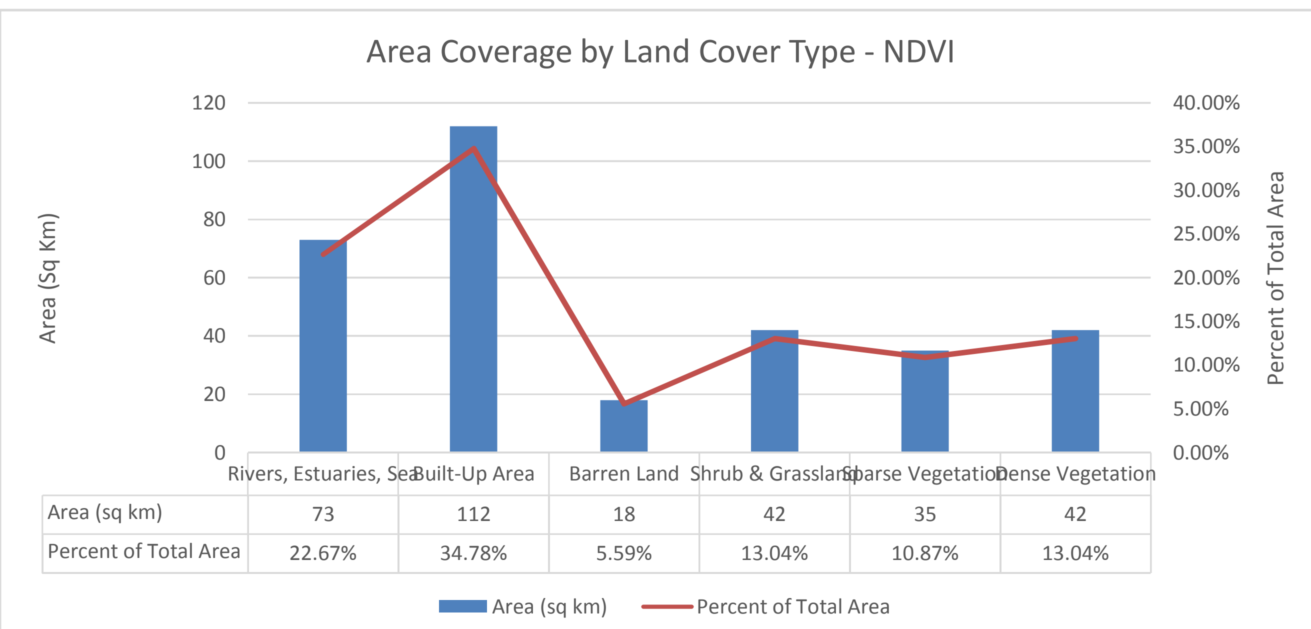

Fig 13: Area Coverage by Land Cover type - NDVI

near-infrared light. The NDVI is a key tool for understanding vegetation dynamics, monitoring drought, predicting agricultural yields, and managing natural resources.

The NDVI map for Mangalore LPA classifies the landscape into several categories based on the vegetation's health and density, which can be crucial for urban and environmental planning.

- **Water Body (NDVI: Very Low Values):** This category indicates areas where there is open water. The NDVI is very low as water bodies reflect little to no near-infrared light. These areas are critical for maintaining urban water supplies and for providing ecological services such as habitat for aquatic organisms.

- **Built-Up Area (NDVI: Low Values):** Urbanized or built-up areas generally show low NDVI values due to the presence of concrete, asphalt, and other materials with high reflectance in the visible wavelengths and low reflectance in the near-infrared. Urban planners need to consider incorporating green spaces into these areas to enhance urban biodiversity, manage urban heat islands, and improve the well-being of residents.

- **Barren Land (NDVI: Low to Moderate Values):** These areas may represent undeveloped land or regions where the vegetation is sparse due to natural or anthropogenic factors. In the context of spatial planning, these areas could be targeted for reforestation or development with an emphasis on sustainability.

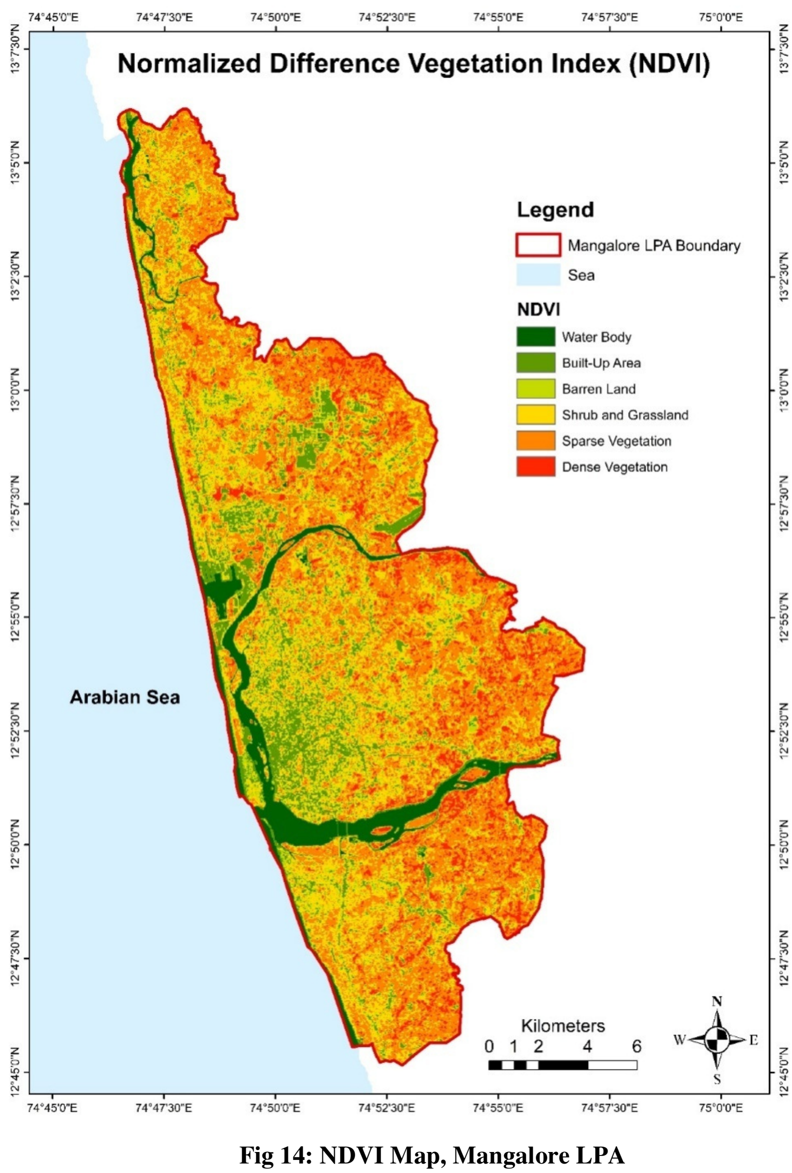

Fig 14: NDVI Map, Mangalore LPA

- **Water Body (NDVI < 0):** Covering an estimated 5% of the LPA, these areas are critical for hydrological and ecological functions. Conservation efforts here are focused on maintaining water quality and protecting habitats. The absence of vegetation reflects in the negative NDVI values, which is characteristic of open water surfaces.
- **Built-Up Area (NDVI 0 - 0.2):** Comprising about 20% of the land, these regions show very poor vegetation health due to urban development. Urban design strategies in these areas could include the creation of urban forests, parks, and green roofs to enhance urban biodiversity, manage stormwater, and mitigate the urban heat island effect.

- **Barren Land (NDVI 0.2 - 0.3):** Making up 10% of the LPA, these lands have poor vegetation health and present opportunities for reforestation or the development of sustainable housing projects with minimal ecological footprint.

TABLE VI
NDVI IMPACTS AND ACTIONS

NDVI Range	Land Cover Type	Area (sq km)	Percent of Total Area	Implications	Recommendations
Water Bodies	Rivers, Estuaries, Sea	73	22.67%	Critical for hydrological regulation, sediment control, and coastal storm protection. Development restrictions mandatory. Restoration of shorelines and connectivity to reduce surge impacts.	Legally designate 50m riparian wetland buffers on all tidal tributaries. Increase stormwater infrastructure requirements for any development in 500-year flood zones. Fund shoreline protection via tiered property surtaxes in high-risk areas.
-0.1 to 0.1	Built-Up Area	112	34.78%	Increased surface runoff impacts from built infrastructure. Spatial plans must require integrated green infrastructure (rain gardens, green roofs, urban tree canopy etc.) to replicate natural hydrology.	Require minimum 30% permeability on commercial sites. Non-permeable public park budgets should equal 2% of transportation budgets. Establish urban forestry plan targeting 35% tree canopy cover in all residential zones by 2050.
0.1 to 0.3	Barren Land	18	5.59%	Contributes to increased surface runoff and reduced carbon sequestration. Spatial policy should target native vegetation restoration in public open spaces.	Convert reclaimed quarries, mines into natural areas to balance development elsewhere. Priority ecological restoration areas designated in comprehensive plans become eligible for offsets markets, conservation funding eligibility.

0.3 to 0.5	Shrub & Grassland	42	13.04%	Provides key ecological services but less than forested areas. Development should be strictly limited with 2:1 open space conservation requirement to maintain regionally native grasslands.	Only allow 20% max imperviousness for new development approvals contingent on recording conservation easements with third party land trusts for the remainder open space. Fertilizer management requirements mandatory.
.5 to 1	Sparse Vegetation	35	10.87%	Scattered forest fragments play an important role in connecting habitats, sediment control, and carbon sequestration. Strict conservation incentives a must through zoning, PDRs, setbacks keyed to climate resilience.	Downzone base densities by 40% in eco-sensitive sparse forest zones. Prohibit clearing of second growth forests. Establish transfer of development rights market targeting receiving areas first. Surtax 10% in sending areas to fund easement acquisition.
>1	Dense Vegetation	42	13.04%	Intact forest systems provide maximal ecosystem services. Highest priority for conservation and development restrictions - 2:1 minimum open space requirement at a minimum.	Prohibit virtually all development, maintain in public ownership. Establish new protected area categorization as "Climate Change Forest Reserve". Levy tiered property taxes increasing with proximity to core reserves to fund payments for private forests.
Total	**-**	**322**	**100%**	**Adaptive spatial planning needed to maintain and expand natural areas critical to climate resilience and carbon regulation.**	**Detailed climate-focused spatial plan updates alongside comprehensive planning process updates essential. Must legitimize climate resilience as key driver. Absent drastic policy updates, severe costs likely.**

- **Shrub and Grassland (NDVI 0.3 - 0.5)**: Representing 15% of the LPA, these areas with moderate vegetation health are important for maintaining biodiversity. They serve as buffer zones between urban and wild areas and can be managed for conservation as well as for recreational purposes.

- **Sparse Vegetation (NDVI 0.5 - 0.7):** Accounting for 25% of the area, these lands with good vegetation health are likely used for agriculture. Monitoring NDVI changes in these areas can help manage and optimize agricultural practices for sustainability and productivity.

- **Dense Vegetation (NDVI > 0.7):** Also covering 25% of the LPA, these areas exhibit excellent vegetation health. They are likely to be dense forests or biodiversity hotspots and should be prioritized for conservation. The high NDVI values indicate robust plant growth and carbon sequestration capabilities, which are vital in combating climate change.

H. Land Use Land Cover – Change Detection

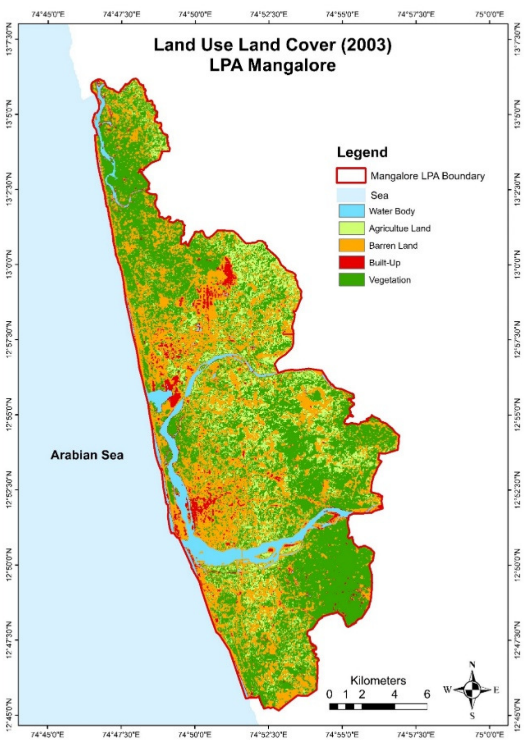

Fig 15: LULC (2003)Map, Mangalore LPA

LULC change detection involves comparing satellite images or maps over different time periods to identify changes in land use and land cover. It is a critical method in urban geography and environmental studies for monitoring urban sprawl, deforestation, agricultural expansion, or transitions in land use due to socio-economic factors.

Technically, change detection analysis employs various remote sensing and Geographic Information System (GIS) techniques. These may include:

- **Normalized Difference Vegetation Index (NDVI):** Utilizing spectral bands to assess changes in green vegetation over time.
- **Supervised Classification:** Applying algorithms to categorize land cover based on training data from known land cover types.
- **Post-Classification Comparison**: Comparing classified images from different years to quantify changes in each LULC category.

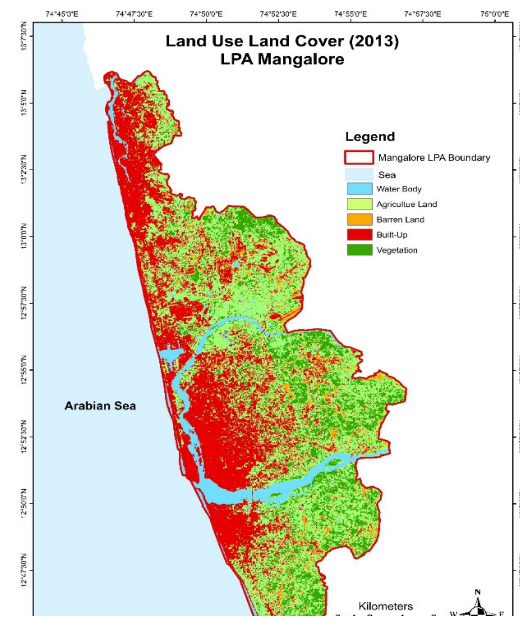

Fig 16: LULC (2013) Map, Mangalore LPA

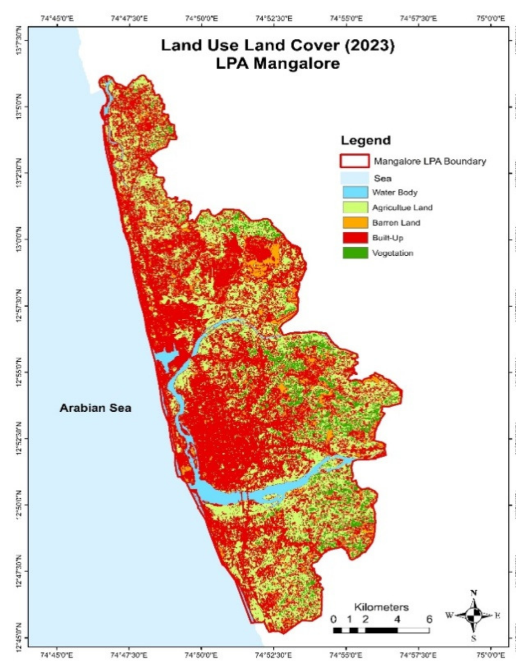

Fig 17: LULC (2023) Map, Mangalore LPA

A thorough analysis would involve generating statistics for each LULC category, including water bodies, agricultural land, barren land, built-up areas, and vegetation. Key trends that might emerge from the 2003-2023 analysis in Mangalore's LPA could include:

- Urban Expansion: An increase in built-up areas may indicate urban growth, often at the expense of agricultural or vegetated lands. This may be driven by population growth and economic development, necessitating sustainable urban planning to balance growth with environmental conservation.
- Agricultural Changes: Shifts in agricultural land can reflect changes in agricultural practices, land important to understand these dynamics to ensure food security and sustainable land management.
- Vegetation Loss or Gain: Changes in vegetated areas can signal environmental degradation or improvement, influenced by deforestation, reforestation, or urban green space initiatives.
- Water Bodies: Alterations in water bodies can be due to natural processes or human activities such as dam construction or land reclamation.

The analysis would be supported by data extracted from the LULC maps and possibly other sources such as census data, agricultural production statistics, and local land use policies. These data points help quantify changes and provide a factual basis for understanding the underlying causes and consequences.

Research articles such as "Land use and land cover change detection through remote sensing approach: A case study of Kodaikanal taluk, India" by Thakur et al., and "Monitoring land cover changes: a comparison of change detection techniques" by Singh, provide insights into methodologies and the significance of change detection in policy formulation.

TABLE VII
LULC IMPLICATIONS, CONSEQUENCES AND POLICY RECOMMENDATIONS

Initial LULC 2003	Final LULC 2023	Area Change (Sq Km)	Implications	Consequences	Policy Recommendations
Agriculture	Built-Up	10.97	Reduced food security, increased flooding	Loss of agricultural GDP, inadequate stormwater infrastructure	- Ag zoning bans on Class 1/2 soils protect food security -Requiring 2:1 open space conservation easement mandate habitat protection with farmland conversion to developed uses
Agriculture	Barren	1.50	Land degradation, soil loss	Increased erosion and nutrient pollution	- Economic incentives for intercropping maintain soil integrity - native vegetation buffers filter agricultural runoff before entering waterways

Barren	Agricultu re	12.42	Reclamation of disturbed land	Reduces pressure on intact habitats	- Habitat restoration developments clean contaminated sites - targets 30% reduction in development outside existing footprints by reclaiming previously disturbed lands first
Barren	Built-Up	45.31	Contaminatio n risk, infrastructure deficits	Health hazards, bloated transportation budgets	- Strict remediation for brownfield redevelopment protects public health - Transit-oriented incentives discourage diffuse suburban type development patterns requiring expanded road infrastructure
Vegetation	Agricultu re	36.08	Deforestation , biodiversity decline	Carbon emissions, lost ecosystem services	- Community forests model prevents agricultural conversion - Reforestation requirements mandate 2 acres replanted per 1 cleared for any agriculture undertaking
Vegetation	Built-Up	24.71	Heat island effects, flash flooding	Localized warming, inadequate stormwater capacity	- Conservation priority habitat incentives (PDRs) steer development - Protected greenways along drainages enhance stormwater and wildlife connectivity
Water Body	Built-Up	2.83	Hydrological disruption	Disturbance of groundwater recharge, well levels	- Expanded riparian wetland buffers protect shorelines and water quality - Stormwater retention basins installed upstream replicate natural hydrology

TABLE VIII
CHANGE DETECTION (2003-2013-2023)

Change Detection (2003-2013-2023)	Area
Agriculture - Agriculture Land - Agriculture Land	11.092384
Agriculture - Agriculture Land - Barren Land	1.498223
Agriculture - Agriculture Land - Built-Up	10.968075
Agriculture - Agriculture Land - Vegetation	0.593594
Agriculture - Barren Land - Agriculture Land	0.360573
Agriculture - Barren Land - Barren Land	0.421211
Agriculture - Barren Land - Built-Up	0.847282
Agriculture - Barren Land - Vegetation	0.031231
Agriculture - Built-Up - Agriculture Land	1.597966
Agriculture - Built-Up - Barren Land	0.583806
Agriculture - Built-Up - Built-Up	6.340266
Agriculture - Built-Up - Vegetation	0.041975
Agriculture - Vegetation - Agriculture Land	5.029546
Agriculture - Vegetation - Barren Land	0.067857
Agriculture - Vegetation - Built-Up	0.546934
Agriculture - Vegetation - Vegetation	1.701715
Agriculture - Water Body - Agriculture Land	0.019188
Agriculture - Water Body - Barren Land	0.001476
Agriculture - Water Body - Built-Up	0.028218
Agriculture - Water Body - Vegetation	0.00037
Barren Land - Agriculture Land - Agriculture Land	12.420969
Barren Land - Agriculture Land - Barren Land	3.737678
Barren Land - Agriculture Land - Built-Up	24.330107
Barren Land - Agriculture Land - Vegetation	0.099397
Barren Land - Agriculture Land - Water Body	0.001093
Barren Land - Barren Land - Agriculture Land	0.516079
Barren Land - Barren Land - Barren Land	2.867301
Barren Land - Barren Land - Vegetation	0.002734
Barren Land - Built-Up - Agriculture Land	2.735685
Barren Land - Built-Up - Barren Land	3.994955
Barren Land - Built-Up - Built-Up	45.314479
Barren Land - Built-Up - Vegetation	0.01098
Barren Land - Built-Up - Water Body	0.015941
Barren Land - Vegetation - Agriculture Land	2.593281
Barren Land - Vegetation - Barren Land	0.062249
Barren Land - Vegetation - Built-Up	0.70937
Barren Land - Vegetation - Vegetation	0.267882
Barren Land - Water Body - Agriculture Land	0.980263
Barren Land - Water Body - Barren Land	0.021291
Barren Land - Water Body - Built-Up	1.429397
Barren Land - Water Body - Vegetation	0.00072
Barren Land - Water Body - Water Body	0.741908
Built-Up - Agriculture Land - Agriculture Land	0.382574
Built-Up - Agriculture Land - Barren Land	0.092901
Built-Up - Agriculture Land - Built-Up	0.980694
Built-Up - Agriculture Land - Vegetation	0.000529
Built-Up - Agriculture Land - Water Body	0.000989
Built-Up - Barren Land - Agriculture Land	0.020507
Built-Up - Barren Land - Barren Land	0.138991
Built-Up - Barren Land - Built-Up	0.344145
Built-Up - Barren Land - Vegetation	0.000561
Built-Up - Barren Land - Water Body	0.00005
Built-Up - Built-Up - Agriculture Land	0.272681
Built-Up - Built-Up - Barren Land	0.372683

Built-Up - Built-Up - Built-Up	6.339788
Built-Up - Built-Up - Vegetation	0.000056
Built-Up - Built-Up - Water Body	0.033858
Built-Up - Vegetation - Agriculture Land	0.027446
Built-Up - Vegetation - Barren Land	0.000966
Built-Up - Vegetation - Built-Up	0.011181
Built-Up - Vegetation - Vegetation	0.001135
Built-Up - Water Body - Agriculture Land	0.301199
Built-Up - Water Body - Barren Land	0.007285
Built-Up - Water Body - Built-Up	0.824392
Built-Up - Water Body - Vegetation	0.000103
Built-Up - Water Body - Water Body	0.382007
Vegetation - Agriculture Land - Agriculture Land	36.0796
Vegetation - Agriculture Land - Barren Land	2.847093
Vegetation - Agriculture Land - Built-Up	30.199157
Vegetation - Agriculture Land - Vegetation	4.116963
Vegetation - Agriculture Land - Water Body	0.000373
Vegetation - Barren Land - Agriculture Land	1.512561
Vegetation - Barren Land - Barren Land	0.937361
Vegetation - Barren Land - Built-Up	2.279586
Vegetation - Barren Land - Vegetation	0.251674
Vegetation - Built-Up - Agriculture Land	9.5126
Vegetation - Built-Up - Barren Land	1.794826
Vegetation - Built-Up - Built-Up	24.705637
Vegetation - Built-Up - Vegetation	0.336959
Vegetation - Built-Up - Water Body	0.012813
Vegetation - Vegetation - Agriculture Land	15.5716
	43
Vegetation - Vegetation - Barren Land	0.173995
Vegetation - Vegetation - Built-Up	1.949909
Vegetation - Vegetation - Vegetation	12.619024
Vegetation - Water Body - Agriculture Land	0.273285
Vegetation - Water Body - Barren Land	0.006614
Vegetation - Water Body - Built-Up	0.272157
Vegetation - Water Body - Vegetation	0.006785
Vegetation - Water Body - Water Body	0.036949
Water Body - Agriculture Land - Agriculture Land	0.056592
Water Body - Agriculture Land - Barren Land	0.014916
Water Body - Agriculture Land - Built-Up	0.089274
Water Body - Agriculture Land - Water Body	0.004685
Water Body - Barren Land - Agriculture Land	0.003406
Water Body - Barren Land - Built-Up	0.002805
Water Body - Built-Up - Agriculture Land	0.121824
Water Body - Built-Up - Barren Land	0.044793
Water Body - Built-Up - Built-Up	1.384535
Water Body - Built-Up - Water Body	0.181918
Water Body - Vegetation - Agriculture Land	0.000202
Water Body - Vegetation - Barren Land	0.003979
Water Body - Vegetation - Built-Up	0.001882
Water Body - Water Body - Agriculture Land	0.345622
Water Body - Water Body - Barren Land	0.01286
Water Body - Water Body - Built-Up	2.828366
Water Body - Water Body - Water Body	14.262362

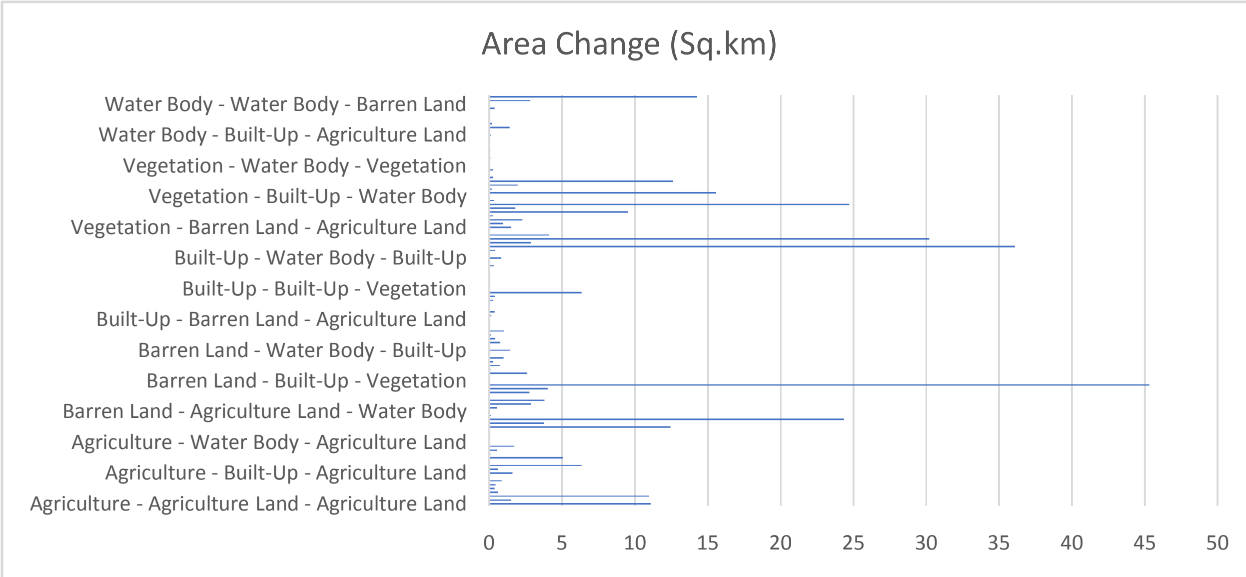

Fig 18: LULC Change Detection Area Change, Mangalore LPA

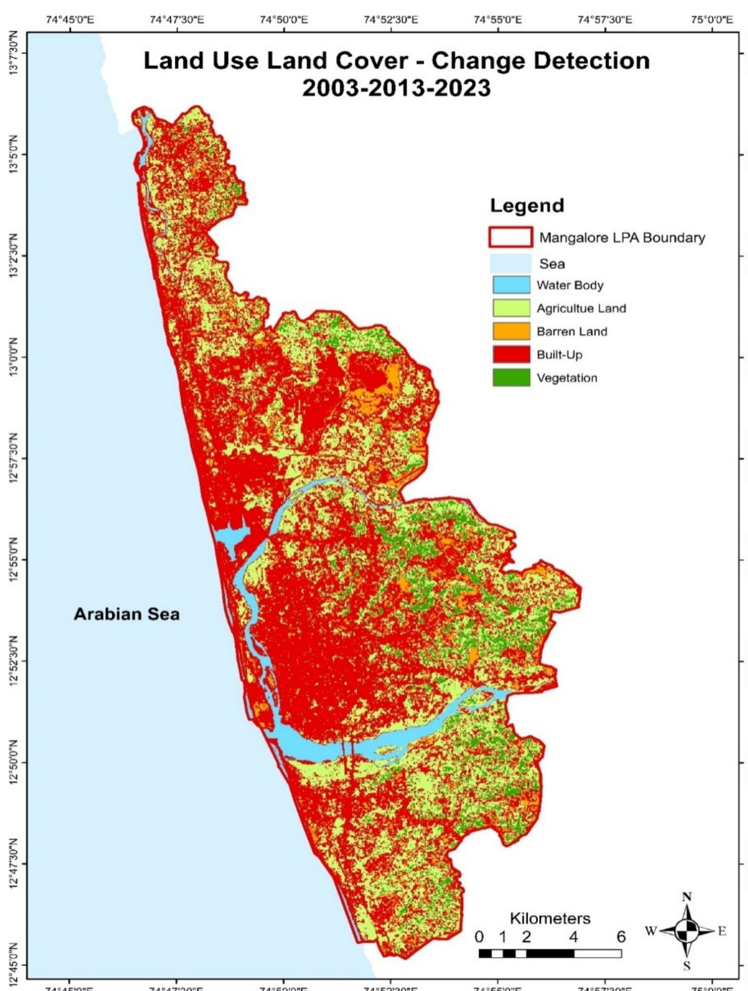

Fig 19: LULC Change Detection Map, Mangalore LPA

I. Flood Susceptibility

The Analytic Hierarchy Process (AHP) is a multi-criteria decision-making technique that has been widely employed in flood susceptibility mapping and risk assessment studies. In the context of Mangalore, India, researchers have utilized AHP to integrate various factors contributing to flood susceptibility and generate spatial representations of risk zones. The Flood Susceptibility map of Mangalore LPA provides a spatial representation of areas with varying degrees of flood risk, categorized from low to very high susceptibility. This classification is derived through the application of the Analytic Hierarchy Process (AHP), a multi-criteria decision-making technique that integrates various contributing factors to flood susceptibility.

Low Susceptibility Areas (Up to 7.5):
These zones exhibit minimal flood risk due to their higher elevation and effective drainage systems. The AHP analysis considers factors such as elevation, slope, land cover, and proximity to water bodies to determine the low susceptibility score. Urban development in these areas can proceed with standard flood mitigation measures, ensuring that new constructions do not impede existing drainage patterns.

Medium Susceptibility Areas (7.5-10.0):
This category includes regions that may experience occasional waterlogging or are adjacent to smaller water bodies. The AHP analysis incorporates factors like soil type, precipitation patterns, and drainage density to assess the medium susceptibility score. Infrastructure planning in these areas should focus on enhanced drainage systems and the incorporation of green spaces that can absorb excess rainfall.

High Susceptibility Areas (10.0-12.5):
Regions within this range are likely to be closer to river banks or low-lying areas that are prone to flooding during heavy rainfall events. The AHP analysis considers factors such as proximity to rivers, flood plains, and historical flood data to determine the high susceptibility score. Urban development in these areas should be highly regulated, with a focus on preserving natural flood plains and implementing advanced flood defense systems.

Very High Susceptibility Areas (More than 12.5):
These are critical zones that require significant attention due to their frequent exposure to floods. The AHP analysis takes into account factors like coastal proximity, tidal influences, and storm surge data to identify these very high susceptibility areas. It is imperative to restrict urban development in these zones and to preserve them as natural buffers, such as wetlands, which can absorb excess water during flood events.

The AHP methodology involves assigning weights to different criteria based on their relative importance in contributing to flood susceptibility. These weights are determined through pairwise comparisons and expert judgments. The process incorporates spatial data from sources like Digital Elevation Models (DEMs), land use/land cover maps, soil maps, and hydrological data. The resulting Flood Susceptibility map serves as a comprehensive decision support tool for urban planners, environmental managers, and policymakers. It provides a data-driven foundation for implementing effective flood risk management strategies, including land use planning, zoning regulations, infrastructure development, and the implementation of structural and non-structural flood mitigation measures. By integrating the AHP analysis with Geographic Information System (GIS) tools, the Flood Susceptibility map of Mangalore LPA can be continuously updated and refined as new data becomes available. This ongoing process ensures that urban development decisions are informed by the most accurate and up-to-date information, ultimately contributing to the creation of a more resilient and sustainable urban landscape.

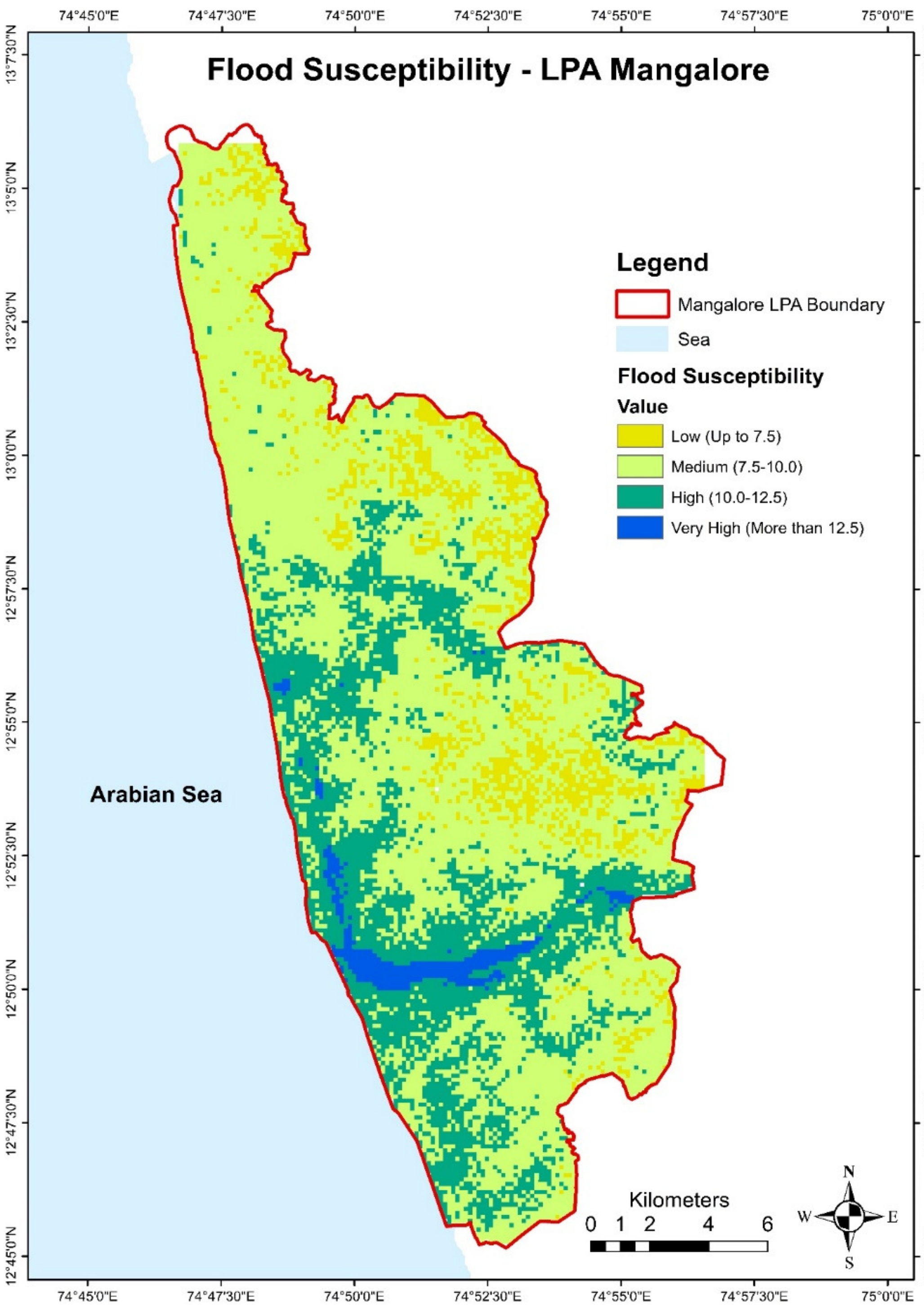

Fig 20: Flood Susceptibility Map, Mangalore LPA

Criterion		Comment	Weights	+/-
1	TWI		13.8%	5.7%
2	Elevation		12.1%	2.7%
3	Slope		9.9%	4.1%
4	Precipitation		13.5%	5.5%
5	LULC		6.6%	3.7%
6	NDVI		5.9%	2.4%
7	Distance from river		14.1%	6.2%
8	Distance from road		5.6%	2.4%
9	Drainage density		9.3%	3.0%
10	Soil type		9.3%	3.0%

Eigenvalue					Lambda:	**10.730**	MRE:	40.4%
Consistency Ratio	0.37	GCI:	0.20	Psi:	-	CR: 5.5%	MRE est	40.3%

Fig 21: AHP Weight Calculation

Matrix		TWI	Elevation	Slope	Precipitation	LULC	NDVI	Distance from river	Distance from road	Drainage density	Soil type	**Normalized Principal Eigenvector**
		1	2	3	4	5	6	7	8	9	10	
TWI	1	1	1	1	1	3	5	1	3	1	1	13.78%
Elevation	2	1	1	1	1	2	3	1	3	1	1	12.07%
Slope	3	1	1	1	1	3	1	1/2	1	1	1	9.90%
Precipitation	4	1	1	1	1	3	2	2	3	1	1	13.45%
LULC	5	1/3	1/2	1/3	1/3	1	1	1/3	3	1	1	6.62%
NDVI	6	1/5	1/3	1	1/2	1	1	1/5	1	1	1	5.87%
Distance from river	7	1	1	2	1/2	3	5	1	3	1	1	14.08%
Distance from road	8	1/3	1/3	1	1/3	1/3	1	1/3	1	1	1	5.59%
Drainage density	9	1	1	1	1	1	1	1	1	1	1	9.32%
Soil type	10	1	1	1	1	1	1	1	1	1	1	9.32%

Fig 22: Weight Calculation Matrix

i	j	Criteria A	B	more important ? A or B	Scale (1-9)
1	2	TWI	Elevation	A	1
1	3		Slope	A	1
1	4		Precipitation	A	1
1	5		LULC	A	3
1	6		NDVI	A	5
1	7		Distance from river	A	1
1	8		Distance from road	A	3
2	3	Elevation	Slope	A	1
2	4		Precipitation	A	1
2	5		LULC	A	2
2	6		NDVI	A	3
2	7		Distance from river	A	1
2	8		Distance from road	A	3
3	4	Slope	Precipitation	A	1
3	5		LULC	A	3
3	6		NDVI	A	1
3	7		Distance from river	B	2
3	8		Distance from road	A	1
4	5	Precipitation	LULC	A	3
4	6		NDVI	A	2
4	7		Distance from river	A	2
4	8		Distance from road	A	3
5	6	LULC	NDVI	A	1
5	7		Distance from river	B	3
5	8		Distance from road	A	3
6	7	NDVI	Distance from river	B	5
6	8		Distance from road	A	1
7	8	Distance from river	Distance from road	A	3

Intensity	Definition	Explanation
1	Equal importance	Two elements contribute equally to the objective
3	Moderate importance	Experience and judgment slightly favor one element over another
5	Strong Importance	Experience and judgment strongly favor one element over another
7	Very strong importance	One element is favored very strongly over another, it dominance is demonstrated in practice
9	Extreme importance	The evidence favoring one element over another is of the highest possible order of affirmation

2,4,6,8 can be used to express intermediate values

Fig 23: Weight Calculation and applying Scale and Importance

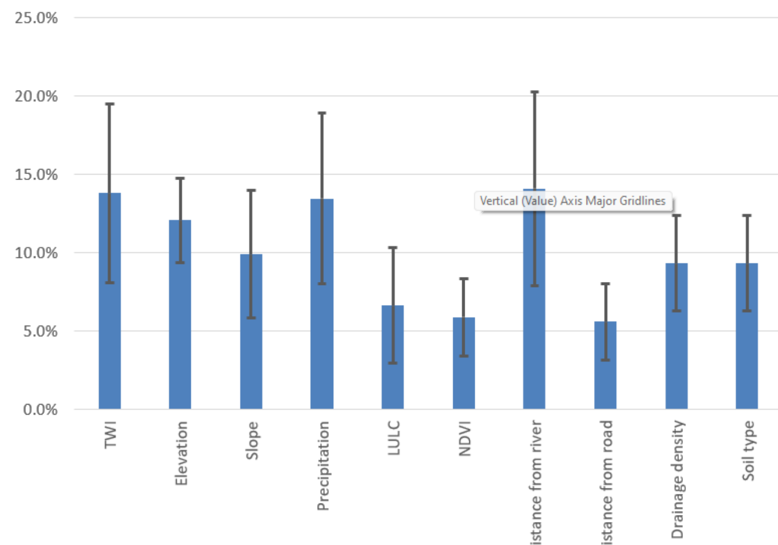

Fig 24: AHP Chart of 10 Parameters

VI. CONCLUSION

This study has systematically assessed flood susceptibility in the urban coastal context of Mangalore using the Analytic Hierarchy Process (AHP) integrated with Geographic Information Systems (GIS). The findings have delineated high-risk areas, offering critical insights for urban planners and policymakers. By incorporating a wide range of factors, including slope, elevation, stream density, precipitation, geology, Topographic Wetness Index (TWI), Normalized Difference Vegetation Index (NDVI), and land use/land cover change dynamics, the research provides a comprehensive understanding of the complex interplay of environmental and anthropogenic factors contributing to flood susceptibility in Mangalore.

The slope analysis revealed that low-lying coastal areas are more prone to flooding, while medium and high-slope regions face challenges related to erosion and landslides. Elevation data highlighted the vulnerability of low-elevation zones to sea-level rise and coastal flooding, emphasizing the need for adaptive planning strategies. Stream density and precipitation patterns underscored the importance of robust stormwater management infrastructure and green spaces to mitigate flood risks. The geological assessment identified areas with unique soil properties and groundwater dynamics that influence infiltration rates and runoff potential.

The Topographic Wetness Index (TWI) proved to be a valuable tool for identifying areas prone to waterlogging and soil saturation, guiding land use decisions and conservation efforts. The Normalized Difference Vegetation Index (NDVI) analysis revealed the critical role of vegetation in regulating surface runoff, carbon sequestration, and ecosystem services, emphasizing the need for strategic conservation and restoration initiatives. Land use/land cover change detection exposed trends such as urban expansion, agricultural shifts, and vegetation loss, underlining the necessity of sustainable land management practices and urban planning that balances development with environmental conservation.

The Analytic Hierarchy Process (AHP) facilitated the integration of these diverse factors, assigning weights based on their relative importance in contributing to flood susceptibility. The resulting flood susceptibility map categorized the study area into low, medium, high, and very high susceptibility zones, providing a visual tool for targeted interventions and resource allocation. The map serves as a foundation for developing risk-informed land use plans, zoning regulations, and infrastructure development strategies that enhance the city's resilience to flooding.

Furthermore, the research highlights the importance of adaptive spatial planning that incorporates projected climate change impacts across various topographic and environmental conditions. It emphasizes the need to maintain and expand natural areas critical to climate resilience and carbon regulation. The study also underscores the significance of stakeholder engagement and participatory approaches in flood risk management, ensuring the involvement of local communities, decision-makers, and experts.

The novelty of this research lies in its integrated approach, combining AHP with GIS to enhance the precision and reliability of flood risk assessment. The methodology demonstrated in this study can be adapted to other regions facing similar challenges, contributing to the growing body of knowledge on flood risk management. However, future research should focus on addressing limitations such as subjectivity in factor weight assignment, limited validation, and the need for more advanced machine learning techniques to improve the accuracy and transferability of the flood susceptibility assessment framework.

In conclusion, this study provides a comprehensive assessment of flood susceptibility in Mangalore, integrating multiple environmental and anthropogenic factors using the Analytic Hierarchy Process (AHP) and Geographic Information Systems (GIS). The findings offer valuable insights for urban planners, policymakers, and stakeholders to develop risk-informed strategies for sustainable urban development, environmental conservation, and climate change adaptation. By prioritizing the protection of natural areas, implementing adaptive spatial planning, and fostering stakeholder collaboration, Mangalore can enhance its resilience to flooding and serve as a model for other coastal cities facing similar challenges in the face of climate change.

VII. ACKNOWLEDGMENT

I would like to express my sincere gratitude to my supervisor, Dr.Bigith V B, for his invaluable guidance, support, and encouragement throughout this research project. His expertise and insights have been instrumental in shaping the direction and quality of this study.

I am also grateful to the faculty and staff of the Department of Urban Planning at Lovely Professional University for providing the necessary resources and facilities to conduct this research. Their support has been crucial in facilitating the smooth progress of this project.

I extend my appreciation to the Mangalore Urban Development Authority and the Disaster Management Department for providing access to essential data and information that formed the foundation of this study.

I would also like to thank my colleagues and fellow researchers for their constructive feedback, stimulating discussions, and moral support throughout this journey. Their camaraderie has made this endeavour a truly enriching experience.

Finally, I am deeply grateful to my family and friends for their unwavering support, patience, and understanding during the course of this research. Their constant encouragement has been a source of strength and motivation.

VIII. REFERENCES

[1] S. Lee and J. Choi, "Landslide susceptibility mapping using GIS and the weight-of-evidence model," *International Journal of Geographical Information Science*, vol. 18, no. 8, pp. 789-814, 2004.

[2] P. Kayastha, M. R. Dhital, and F. De Smedt, "Application of the analytical hierarchy process (AHP) for landslide susceptibility mapping: a case study from the Tinau watershed, west Nepal," *Computers & Geosciences*, vol. 52, pp. 398-408, 2013.

[3] T. L. Saaty, "A scaling method for priorities in hierarchical structures," *Journal of Mathematical Psychology*, vol. 15, no. 3, pp. 234-281, 1977.

[4] J. Malczewski, "GIS-based multicriteria decision analysis: a survey of the literature," *International Journal of Geographical Information Science*, vol. 20, no. 7, pp. 703-726, 2006.

[5] M. S. Tehrany, B. Pradhan, and M. N. Jebur, "Flood susceptibility mapping using a novel ensemble weights-of-evidence and support vector machine models in GIS," *Journal of Hydrology*, vol. 512, pp. 332-343, 2014.

[6] R. C. Sidle and H. Ochiai, *Landslides: processes, prediction, and land use*. Washington, D.C.: American Geophysical Union, 2006.

[7] O. F. Althuwaynee, B. Pradhan, and S. Lee, "Application of an evidential belief function model in landslide susceptibility mapping," *Computers & Geosciences*, vol. 44, pp. 120-135, 2012.

[8] B. T. Pham, D. Tien Bui, I. Prakash, and M. B. Dholakia, "Hybrid integration of Multilayer Perceptron Neural Networks and machine

learning ensembles for landslide susceptibility assessment at Himalayan area (India) using GIS," *Catena*, vol. 149, pp. 52-63, 2017.
[9] P. V. Gorsevski, P. Jankowski, and P. E. Gessler, "A heuristic approach for mapping landslide hazard by integrating fuzzy logic with analytic hierarchy process," *Control and Cybernetics*, vol. 35, no. 1, pp. 121-146, 2006.
[10] Y. Hong, H. R. Pourghasemi, and Z. S. Pourtaghi, "Landslide susceptibility assessment in Lianhua County (China): a comparison between a random forest data mining technique and bivariate and multivariate statistical models," *Geomorphology*, vol. 259, pp. 105-118, 2016.
[11] A. Yalcin, S. Reis, A. C. Aydinoglu, and T. Yomralioglu, "A GIS-based comparative study of frequency ratio, analytical hierarchy process, bivariate statistics and logistics regression methods for landslide susceptibility mapping in Trabzon, NE Turkey," *Catena*, vol. 85, no. 3, pp. 274-287, 2011.
[12] S. Lee, J.-H. Ryu, J.-S. Won, and H.-J. Park, "Determination and application of the weights for landslide susceptibility mapping using an artificial neural network," *Engineering Geology*, vol. 71, no. 3-4, pp. 289-302, 2004.
[13] M. S. Tehrany, B. Pradhan, S. Mansor, and N. Ahmad, "Flood susceptibility assessment using GIS-based support vector machine model with different kernel types," *Catena*, vol. 125, pp. 91-101, 2015.
[14] G. Weirich and T. Blesius, "Comparison of satellite and air photo-based landslide susceptibility maps," *Geomorphology*, vol. 87, no. 4, pp. 352-364, 2007.
[15] E. F. Lambin and D. Ehrlich, "Land-cover changes in sub-Saharan Africa (1982–1991): application of a change index based on remotely sensed surface temperature and vegetation indices at a continental scale," *Remote Sensing of Environment*, vol. 61, no. 2, pp. 181-200, 1997.
[16] B. Pradhan, "Flood susceptible mapping and risk area delineation using logistic regression, GIS and remote sensing," *Journal of Spatial Hydrology*, vol. 9, no. 2, pp. 1-18, 2009.
[17] D. Tien Bui, B. Pradhan, O. Lofman, I. Revhaug, and O. B. Dick, "Spatial prediction of landslide hazards in Hoa Binh province (Vietnam): a comparative assessment of the efficacy of evidential belief functions and fuzzy logic models," *Catena*, vol. 96, pp. 28-40, 2012.
[18] J. C. Villagran de Leon, "Vulnerability: a conceptual and methodological review," *Studies of the University: Research, Counsel, Education*, vol. 4, no. 4, pp. 1-84, 2006.
[19] B. Pradhan and S. Lee, "Landslide risk analysis using artificial neural network model focusing on different training sites," *International Journal of Physical Sciences*, vol. 4, no. 1, pp. 1-15, 2009.
[20] K. Khosravi, S.-H. Cheng, E. Sartohoun, A. A. Adeleke, and B. Pradhan, "A comparative study of logistic model tree, naive Bayes and random forest for landslide susceptibility mapping," *Geomatics, Natural Hazards and Risk*, vol. 9, no. 1, pp. 1051-1072, 2018.
[21] B. Pradhan, "A comparative study on the predictive ability of the decision tree, support vector machine and neuro-fuzzy models in landslide susceptibility mapping using GIS," *Computers & Geosciences*, vol. 51, pp. 350-365, 2013.
[22] J. P. Wilson and J. C. Gallant, Eds., *Terrain analysis: principles and applications*. John Wiley & Sons, 2000.
[23] I. D. Moore, R. B. Grayson, and A. R. Ladson, "Digital terrain modelling: a review of hydrological, geomorphological, and biological applications," *Hydrological Processes*, vol. 5, no. 1, pp. 3-30, 1991.
[24] T. Glade, M. Crozier, and P. Smith, "Applying probability determination to refine landslide-triggering rainfall thresholds using an empirical "Antecedent Daily Rainfall Model"," *Pure and Applied Geophysics*, vol. 157, no. 6-8, pp. 1059-1079, 2000.
[25] O. Rahmati, H. R. Pourghasemi, and H. Zeinivand, "Flood susceptibility mapping using frequency ratio and weights-of-evidence models in the Golastan Province, Iran," *Geocarto International*, vol. 31, no. 1, pp. 42-70, 2016.
[26] O. Rahmati and H. R. Pourghasemi, "Identification of critical flood prone areas in data-scarce and ungauged regions: a comparison of three data mining models," *Water Resources Management*, vol. 31, no. 5, pp. 1473-1487, 2017.
[27] M. Sahana and H. Patel, "Application of frequency ratio and Shannon's entropy models for landslide hazard assessment of Rudraprayag district, Uttarakhand, India," *Journal of Mountain Science*, vol. 17, no. 12, pp. 3030-3044, 2020.
[28] B. Pradhan, S. Lee, and M. F. Buchroithner, "A GIS-based back-propagation neural network model and its cross-application and validation for landslide susceptibility analyses," *Computers, Environment and Urban Systems*, vol. 34, no. 3, pp. 216-235, 2010.
[29] C. J. Van Westen, E. Castellanos, and S. L. Kuriakose, "Spatial data for landslide susceptibility, hazard, and vulnerability assessment: an overview," *Engineering Geology*, vol. 102, no. 3-4, pp. 112-131, 2008.
[30] A. Yalcin and F. Bulut, "Landslide susceptibility mapping using GIS and digital photogrammetric techniques: a case study from Ardesen (NE-Turkey)," *Natural Hazards*, vol. 41, no. 1, pp. 201-226, 2007.
[31] M. L. Suzen and V. Doyuran, "A comparison of the GIS based landslide susceptibility assessment methods: multivariate versus bivariate," *Environmental Geology*, vol. 45, no. 5, pp. 665-679, 2004.
[32] C.-Y. Yeh, B. Pradhan, M. Abha Bafna, and A. A. Maulud, "Assessment of landslide susceptibility using ensemble of functional trees and forest by penalizing attributes (FPA) models," *Remote Sensing*, vol. 13, no. 22, p. 4625, 2021.
[33] S. Segoni, L. Piciullo, and S. L. Gariano, "A review of the recent literature on rainfall thresholds for landslide occurrence," *Landslides*, vol. 15, no. 8, pp. 1483-1501, 2018.
[34] J. N. Goetz, A. Brenning, H. Petschko, and P. Leopold, "Evaluating machine learning and statistical prediction techniques for landslide susceptibility modeling," *Computers & Geosciences*, vol. 81, pp. 1-11, 2015.
[35] A. Getahun, K. V. Suryabhagavan, T. Balakrishnan Nair, and R. Srinivasan, "Landslide susceptibility mapping using analytical hierarchical process and geographic information system in Gish Abay watershed, Lake Tana sub-basin, Northwestern Ethiopia," *Spatial Information Research*, vol. 29, no. 6, pp. 935-951, 2021.
[36] A. I. Kanungo, "Carrying capacity for Himalayan towns: a case of Mussoorie," *ITPI Journal*, vol. 5, no. 3, pp. 55-62, 2008.
[37] X. J. Shi, A. Kasperson, and R. Kasperson, "Coping with and Managing Vulnerability to Environmental and Technological Hazards," *Coping with Global Environmental Change, Disasters and Security*, pp. 1205-1223, 2011.
[38] J. M. Keller, M. R. Gray, and J. A. Givens, "A fuzzy K-nearest neighbor algorithm," *IEEE Transactions on Systems, Man, and Cybernetics*, vol. SMC-15, no. 4, pp. 580-585, 1985.
[39] J. Li, "Landslide hazard assessment using fuzzy logic and artificial neural network models," *Journal of Mountain Science*, vol. 15, no. 3, pp. 648-659, 2018.
[40] K. S. Lee, S. Kim, and J. Kim, "Assessment of regional flood frequency in South Korea using L-moment," *KSCE Journal of Civil Engineering*, vol. 11, no. 1, pp. 49-55, 2007.
[41] A. Burton and J. Bathurst, "Physically based modelling of shallow landslide sediment yield at a catchment scale," *Environmental Geology*, vol. 35, no. 2, pp. 89-99, 1998.
[42] Z. M. Yaseen *et al.*, "Flash flood susceptibility modeling using new ensemble and deep learning models," *IEEE Access*, vol. 9, pp. 2233-2254, 2020.
[43] J. Coe, W. Ellis, J. Godt, W. Savage, J. Savage, J. Michael, J. Kibler, P. Powers, D. Lidke, and S. Debray, "Seasonal movement of the Slumgullion landslide determined from Global Positioning System surveys and field instrumentation, July 1998–March 2002," *Engineering Geology*, vol. 68, no. 1-2, pp. 67-101, 2003.
[44] F. Guzzetti, A. Carrara, M. Cardinali, and P. Reichenbach, "Landslide hazard evaluation: a review of current techniques and their application in a multi-scale study, Central Italy," *Geomorphology*, vol. 31, no. 1-4, pp. 181-216, 1999.
[45] A. Yalcin, S. Reis, A. C. Aydinoglu, and T. Yomralioglu, "A GIS-based comparative study of frequency ratio, analytical hierarchy process, bivariate statistics and logistics regression methods for landslide susceptibility mapping in Trabzon, NE Turkey," *Catena*, vol. 85, no. 3, pp. 274-287, 2011.
[46] O. Rahmati, A. Haghizadeh, H. R. Pourghasemi, and F. Noormohamadi, "Gully erosion susceptibility mapping: the role of GIS-based bivariate

statistical models and their comparison," *Natural Hazards*, vol. 82, no. 2, pp. 1231-1258, 2016.

[47] F. Gutierrez, M. Soldati, F. Audemard, and D. Balteanu, "Recent advances in landslide investigation: issues and perspectives," *Geomorphology*, vol. 124, no. 3-4, pp. 95-101, 2010.

[48] T. R. Martha, P. Roy, K. B. Khanna, K. V. Kumar, P. G. Rao, and R. Krishnamurthy, "Debris flow hazard and risk assessment using high-resolution satellite data, GPS survey and numerical modeling," *Remote Sensing*, vol. 11, no. 20, p. 2346, 2019.

[49] F. Wang, H. Xu, P. Lu, and H. Wang, "Landslide susceptibility mapping using random forest and the index of entropy method," *Neural Computing and Applications*, vol. 34, no. 1, pp. 345-360, 2022.

[50] B. Dixon and J. Earls, "Resample or not?! Effects of resolution of DEMs in watershed modeling," *Hydrological Processes: An International Journal*, vol. 23, no. 12, pp. 1714-1724, 2009.

[51] G. Metternicht, L. Hurni, and R. Gogu, "Remote sensing of landslides: An analysis of the potential contribution to geo-spatial systems for hazard assessment in mountainous environments," *Remote Sensing of Environment*, vol. 98, no. 2-3, pp. 284-303, 2005.

[52] J. Goetz, R. H. Guthrie, and A. Brenning, "Integrating physical and empirical landslide susceptibility models using generalized additive models," *Geomorphology*, vol. 129, no. 3-4, pp. 376-386, 2011.

[53] F. Ponziani, C. Pandolfo, M. Stelluti, N. Berni, L. Brocca, and T. Morassi, "Assessment of rainfall thresholds and soil moisture modeling for operational hydrogeological risk prevention in the Umbria region (central Italy)," Landslides, vol. 9, no. 2, pp. 229-237, 2012.

[54] S. Lee and B. Pradhan, "Landslide hazard mapping at Selangor, Malaysia using frequency ratio and logistic regression models," Landslides, vol. 4, no. 1, pp. 33-41, 2007.

[55] S. Segoni, A. Battistini, G. Rossi, A. Rosi, D. Lagomarsino, F. Catani, S. Moretti, and N. Casagli, "Technical note: an operational landslide early warning system at regional scale based on space-time-variable rainfall thresholds," Natural Hazards and Earth System Sciences, vol. 15, no. 4, pp. 853-861, 2015.

[56] T. Glade, "Landslide occurrence as a response to land use change: a review of evidence from New Zealand," Catena, vol. 51, no. 3-4, pp. 297-314, 2003.

[57] F. C. Dai and C. F. Lee, "Landslide characteristics and slope instability modeling using GIS, Lantau Island, Hong Kong," Geomorphology, vol. 42, no. 3-4, pp. 213-228, 2002.

[58] H. A. Nefeslioglu, C. Gokceoglu, and H. Sonmez, "An assessment on the use of logistic regression and artificial neural networks with different sampling strategies for the preparation of landslide susceptibility maps," Engineering Geology, vol. 97, no. 3-4, pp. 171-191, 2008.

[59] J. Corominas et al., "Recommendations for the quantitative analysis of landslide risk," Bulletin of Engineering Geology and the Environment, vol. 73, no. 2, pp. 209-263, 2014.

[60] M. Bordoni et al., "Landslide susceptibility mapping of the Oltrepò Pavese (northern Italy) using ensemble of advanced machine learning and statistical models," Remote Sensing, vol. 14, no. 9, p. 2145, 2022.

[61] J.-S. Won and S. Lee, "Application of logistic regression model and its validation for landslide susceptibility mapping using GIS and remote sensing data," International Journal of Remote Sensing, vol. 26, no. 7, pp. 1477-1491, 2005.

[62] H. B. Bui, D. T. Bui, N. D. Hoang, and N.-D. Hoang, "A spatial decision support system for sustainable hydropower development in the Lao Cai province, Vietnam," Sustainability, vol. 13, no. 10, p. 5503, 2021.

[63] A. Manconi, D. Giordan, P. Allasia, F. Baldo, and D. Lollino, "Surface displacements following the Mw 6.3 L'Aquila earthquake: One year of continuous monitoring via Robotized Total Station," Italian Journal of Geosciences, vol. 131, no. 3, pp. 403-409, 2012.

[64] B. E. Montz and G. A. Tobin, "Livin' large with levees: lessons learned and lost," Natural Hazards Review, vol. 9, no. 3, pp. 150-157, 2008.

[65] L. Lombardo, H. Bakka, H. Tanyas, C. van Westen, P. Mai, and R. Huser, "Geostatistical modeling to capture seismic-shaking patterns from earthquake-induced landslides," Journal of Geophysical Research: Earth Surface, vol. 124, no. 7, pp. 1958-1980, 2019.

[66] T. W. J. Van Asch, J. Buma, and L. P. H. Van Beek, "A view on some hydrological triggering systems in landslides," Geomorphology, vol. 30, no. 1-2, pp. 25-32, 1999.

[67] C. Chreties, L. Dondo, G. Decia, G. Silveira, and L. Silveira, "Flood risk analysis in Artigas city, Uruguay: hydrological and hydraulic assessment of the Cuareim river," Natural Hazards, vol. 106, no. 1, pp. 99-117, 2021.

[68] B. T. Pham, A. Jaafari, M. Avand, N. Al-Ansari, T. Dinh Du, H. P. H. Yen, T. V. Phong, D. H. Nguyen, H. V. Le, I. Prakash, P. T. T. Ngo, and T. T. Tuyen, "Performance evaluation of artificial intelligence methods for forest fire modeling and prediction," Symmetry, vol. 12, no. 6, p. 1022, 2020.

[69] S. Beguería, "Changes in land cover and shallow landslide activity: a case study in the Spanish Pyrenees," Geomorphology, vol. 74, no. 1-4, pp. 196-206, 2006.

[70] A. Odukoya, R. Folorunso, and M. Ayolabi, "Geoenvironmental assessment of flood prone areas using remote sensing and geographic information system techniques," Journal of Applied Sciences & Environmental Management, vol. 23, no. 7, pp. 1397-1405, 2019.

[71] T. J. Ballesteros Canovas, M. Stoffel, and M. Bollschweiler, "Combination of tree-ring records and geomorphic mapping to assess variations in debris-flow frequency in Val Ferret (Eastern Italian Alps)," Geophysical Research Abstracts, vol. 12, p. 2935, 2010.

[72] S. Grimaldi, V. Teles, and R. L. Bras, "Sensitivity of a physically based method for terrain interpolation to initial conditions and its conditioning on stream location," Earth Surface Processes and Landforms: The Journal of the British Geomorphological Research Group, vol. 29, no. 5, pp. 587-597, 2004.

[73] G. Wang and K. Sassa, "Pore-pressure generation and movement of rainfall-induced landslides: effects of grain size and fine-particle content," Engineering Geology, vol. 69, no. 1-2, pp. 109-125, 2003.

[74] D. Hillel, Introduction to environmental soil physics. Elsevier, 2003.

[75] P. Mazzanti and F. Bozzano, "An equivalent fluid/equivalent medium approach for the numerical simulation of coastal landslides propagation: theory and case studies," Natural hazards, vol. 50, no. 3, pp. 437-463, 2009.

[76] A. Carrara, M. Cardinali, F. Guzzetti, and P. Reichenbach, "GIS technology in mapping landslide hazard," in Geographical information systems in assessing natural hazards. Springer, 1995, pp. 135-175.

[77] S. G. Evans, "Landslide damming in the Cordillera of western Canada," Landslide Dams: Processes, Risk, and Mitigation, pp. 111-130, 1986.

[78] O. Korup, "Recent research on landslide dams-a literature review with special attention to New Zealand," Progress in Physical Geography, vol. 26, no. 2, pp. 206-235, 2002.

[79] A. J. Remaître and T. W. J. Van Asch, "Influences on the mobility of debris flows and the consequences for hazard assessment," in Debris-flow hazards and related phenomena. Springer, 2005, pp. 307-322.

[80] T. Takahashi, "Estimation of potential debris flows and their hazardous zones: soft countermeasures for a disaster," Journal of Natural Disaster Science, vol. 3, no. 1, pp. 57-89, 1981.

[81] X. Zhu, Q. Xu, and G. Qi, "A present review on the assessment of landslide hazard: a case study in China," Natural Hazards, vol. 108, no. 3, pp. 2371-2394, 2021.

[82] T. Fernández, C. Irigaray, R. E. Hamdouni, and J. Chacón, "Methodology for landslide susceptibility mapping by means of a GIS. Application to the Contraviesa area (Granada, Spain)," Natural Hazards, vol. 30, no. 3, pp. 297-308, 2003.

[83] T. B. Cheng, G. Liu, K. B. Zhang, and H. Gao, "Debris flow risk assessment under climate change: a case study of Qipan Gully in Wenchuan Area," IOP Conference Series: Earth and Environmental Science, vol. 189, no. 3, p. 032033, 2018.

[84] A. K. Saha, R. P. Gupta, I. Sarkar, M. K. Arora, and E. Csaplovics, "An approach for GIS-based statistical landslide susceptibility zonation—with a case study in the Himalayas," Landslides, vol. 2, no. 1, pp. 61-69, 2005.

[85] M. S. Tehrany, B. Pradhan, and M. N. Jebur, "Spatial prediction of flood susceptible areas using rule-based decision tree (DT) and a novel ensemble bivariate and multivariate statistical models in GIS," Journal of Hydrology, vol. 504, pp. 69-79, 2013.

[86] K.-T. Chang, S.-H. Chiang, and M.-L. Hsu, "Modeling typhoon- and earthquake-induced landslides in a mountainous watershed using logistic regression," Geomorphology, vol. 89, no. 3-4, pp. 335-347, 2007.

[87] S. Sreekumar, "Techniques for slope stability analysis: site specific studies for landslides hazard zonation," PhD thesis, p. 239, 2009.

[88] C. Van Westen, M. Kappes, B. Luna, P. Frigerio, T. Glade, and J.-P. Malet, "Medium-scale multi-hazard risk assessment of gravitational processes," in Mountain risks: from prediction to management and governance. Springer, 2014, pp. 201-231.

[89] H. Hong, B. Pradhan, C. Xu, and D. Tien Bui, "Spatial prediction of landslide hazard at the Yihuang area (China) using two-class kernel logistic regression, alternating decision tree and support vector machines," Catena, vol. 133, pp. 266-281, 2015.

[90] M. A. Siddiqui and V. Maruthi Srinivas, "Flash flood risk assessment using morphological parameters: a case study of Meenachil River Basin, Kerala, India," Natural Hazards, vol. 107, no. 1, pp. 297-327, 2021.

[91] N. Santangelo, L. Daunis-i Estadella, A. Di Crescenzo, E. Di Donato, S. Di Martire, and A. Santo, "Topographic predictors of susceptibility to alluvial fan flooding, Southern Apennines," Earth Surface Processes and Landforms, vol. 37, no. 8, pp. 803-817, 2012.

[92] P. Tarolli and D. G. Tarboton, "A new method for determination of most likely landslide initiation points and the evaluation of digital terrain model scale in terrain stability mapping," Hydrology and Earth System Sciences, vol. 10, no. 5, pp. 663-677, 2006.

[93] M. T. Rahman and M. S. Islam, "Landslide susceptibility mapping of Rangamati hill tracts using GSI and AHP techniques: A study on Rangamati Sadar, Kawkhali, Bilaichhari, Langadu and Nannerchar Upazilas of Bangladesh," Asian Journal of Geographical Research, pp. 1-15, 2022.

[94] R. Dutta, T. Aryal, and R. K. Rai, "Flood inundation mapping of Jalpaiguri Sadar, West Bengal, India using HEC-RAS 1D-2D couple model," Stochastic Environmental Research and Risk Assessment, vol. 36, no. 8, pp. 2735-2754, 2022.

[95] R. Vandine, D. Moore, L. Wise, E. Vanbuskirk, and G. Gerath, "Technical terms and methods," Geological Fieldwork, vol. 2002, pp. 1-10, 2003.

[96] A. J. Das, K. Szabó, and M. K. Jha, "Modeling of debris flow and the assessment of its impact on check dams in a Himalayan watershed using GIS and the DAN3D approach," Natural Hazards, vol. 116, no. 3, pp. 1521-1544, 2023.

[97] P. Vorpahl, H. Elsenbeer, M. Märker, and B. Schröder, "How can statistical models help to determine driving factors of landslides?," Ecological Modelling, vol. 239, pp. 27-39, 2012.

[98] V. R. Gaddam, T. Kulkarni, S. Singh, and G. Mathur, "Assessment of Flood Susceptibility of Coal Mines in India Using Artificial Neural Network and Analytical Hierarchy Process Approaches," Journal of Hydrologic Engineering, vol. 26, no. 8, p. 05021018, 2021.

[99] R. K. Magar, K. E. Sachan, and M. Ahmad, "Landslide susceptibility mapping using remote sensing and GIS: a case study of Kashmir Himalayas," International Journal of Innovative Technology and Exploring Engineering, vol. 8, no. 12, pp. 3809-3814, 2019.

[100] S. Shit and D. Bera, "Applying Geospatial Technologies in Flood Vulnerability Zonation and Risk Management along the Lower Luni Basin, Barmer, Rajasthan," Bulletin of Environmental and Scientific Research, vol. 11, no. 1, pp. 45-57, 2022.